

AD-A102 347

ISRAEL INST OF METALS HAIFA

F/G 11/4

SOLID PARTICLE EROSION PROCESSES IN COATINGS AND COMPOSITE MATE--ETC(U)

MAY 81 J ZAHAVI

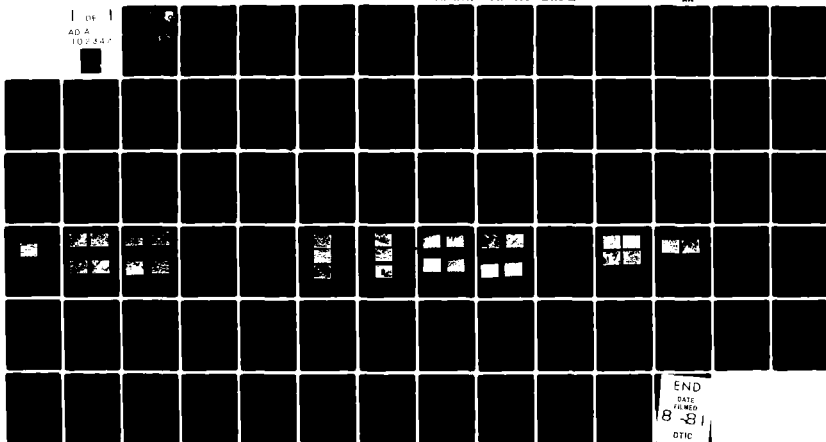
AFOSR-80-0140

UNCLASSIFIED

AFWAI-TD-R1-4024

AM

1 OF 1
AD A
107347



END
DATE
FILMED
8-81
DTIC

AD A102347

AFWAL-TR-81-4024

LEVEL II

2



SOLID PARTICLE EROSION PROCESSES IN
COATINGS AND COMPOSITE MATERIALS

Joseph Zahavi
Israel Institute of Metals
Technion
Haifa, Israel

DTIC
ELECTE
S AUG 03 1981 D
E

May 1981

Technical Report for period April 1980 - March 1981

Approved for public release; distribution unlimited

DTIC FILE COPY

MATERIALS LABORATORY
AIR FORCE WRIGHT AERONAUTICAL LABORATORIES
AIR FORCE SYSTEMS COMMAND
WRIGHT-PATTERSON AIR FORCE BASE, OHIO 45433


81 7 31 065


NOTICE

When Government drawings, specifications, or other data are used for any purpose other than in connection with a definitely related Government procurement operation, the United States Government thereby incurs no responsibility nor any obligation whatsoever; and the fact that the government may have formulated, furnished, or in any way supplied the said drawings, specifications, or other data, is not to be regarded by implication or otherwise as in any manner licensing the holder or any other person or corporation, or conveying any rights or permission to manufacture use, or sell any patented invention that may in any way be related thereto.

This report has been reviewed by the Office of Public Affairs (ASD/PA) and is releasable to the National Technical Information Service (NTIS). At NTIS, it will be available to the general public, including foreign nations.

This technical report has been reviewed and is approved for publication.


G. F. SCHMITT, JR.
Project Engineer


W. C. KESSLER, Chief
Coatings & Thermal Protective
Materials Branch
Nonmetallic Materials Division

FOR THE COMMANDER


F. D. CHERRY, Chief
Nonmetallic Materials Division

"If your address has changed, if you wish to be removed from our mailing list, or if the addressee is no longer employed by your organization please notify AFWAL/MLBE, W-PAFB, OH 45433 to help us maintain a current mailing list".

Copies of this report should not be returned unless return is required by security considerations, contractual obligations, or notice on a specific document.

UNCLASSIFIED

SECURITY CLASSIFICATION OF THIS PAGE (When Data Entered)

REPORT DOCUMENTATION PAGE		READ INSTRUCTIONS BEFORE COMPLETING FORM
1. REPORT NUMBER AFWAL/TR-81-4024	2. GOVT ACCESSION NO. AD-A702 347	3. RECIPIENT'S CATALOG NUMBER
4. TITLE (and Subtitle) SOLID PARTICLE EROSION PROCESSES IN COATINGS AND COMPOSITES - Materials	5. TYPE OF REPORT & PERIOD COVERED Interim Report April 1980 - March 1981	6. PERFORMING ORG. REPORT NUMBER
7. AUTHOR(s) Joseph/Zahavi	8. CONTRACT OR GRANT NUMBER(s) AFOSR-80-0140	
9. PERFORMING ORGANIZATION NAME AND ADDRESS Israel Institute of Metals Technion Haifa, Israel	10. PROGRAM ELEMENT, PROJECT, TASK AREA & WORK UNIT NUMBERS 62102F, 2422, 242201, 24220122	
11. CONTROLLING OFFICE NAME AND ADDRESS AFOSR (PKN) Bolling AFB, DC 20332	12. REPORT DATE May 1981	
14. MONITORING AGENCY NAME & ADDRESS (if different from Controlling Office) Materials Laboratory (AFWAL/MLBE) Air Force Wright Aeronautical Laboratories Wright-Patterson Air Force Base, Ohio 45433	15. SECURITY CLASS. (of this report) UNCLASSIFIED	
16. DISTRIBUTION STATEMENT (of this Report) Approved for public release; distribution unlimited.		
17. DISTRIBUTION STATEMENT (of the abstract entered in Block 20, if different from Report)		
18. SUPPLEMENTARY NOTES		
19. KEY WORDS (Continue on reverse side if necessary and identify by block number) Solid particle impact erosion polyurethane fluorocarbon elastomeric coatings composites		
20. ABSTRACT (Continue on reverse side if necessary and identify by block number) Solid particle impingement erosion of uncoated composite materials of quartz-polyimide, glass-epoxy and quartz-polybutadiene constructions and of three protective coatings; a hard MIL-C-83286 polyurethane, an elastomeric AF-C-VBW-15-15 fluorocarbon, has been investigated utilizing natural Mediterranean Sea sand. Environmental parameters of impact angle (15 to 90) and sand weight impacted (200, 400 and 600 g) have been examined and materials response was characterized by weight loss, surface roughness and surface morphology.		

DD FORM 1 JAN 73 1473 EDITION OF 1 NOV 65 IS OBSOLETE

UNCLASSIFIED
SECURITY CLASSIFICATION OF THIS PAGE (When Data Entered)

393650

514

UNCLASSIFIED

SECURITY CLASSIFICATION OF THIS PAGE(When Data Entered)

While progressive weight loss was observed on all materials with increasing weight of sand impacted, one glass-epoxy composite exhibited half an order of magnitude less erosion than the other composites; this is attributed to its better adhesion between the matrix and fibers, higher percentage of fiber loading, and lower porosity. This glass-epoxy composite exhibited semi-ductile erosion behavior with a maximum weight loss at 45-60° while the other eroded in a brittle manner with a maximum at 75-90°.

The erosion process in these composites consisted of the following sequence: (1) erosion and local material removal in the resin zones; (2) erosion in the fiber zones associated with breakage of fibers due to bending failure of unsupported sections where resin beneath had been removed; and (3) erosion of the interface zones between the fibers and the adjacent matrix.

In all coatings investigated, erosion rate (i.e., target weight loss) decreased with the increase of the impact angle. Maximum weight loss was found at 30° while minimum value of weight loss was found at normal impact angle. However, in elastomeric MIL-C-83231 polyurethane and AF-C-VBW-15-15 fluorocarbon coatings, erosion rate was found to be independent of impact angle at the range of 45° to 90°.

A progressive increase in target coating weight loss with amount of sand impacted was found in MIL-C-83286 polyurethane coatings at constant impact angles. However, in MIL-C-83231 polyurethane and AF-C-VBW-15-15 fluorocarbon coatings, erosion rate (i.e., target weight change) was found to be independent of weight of sand impacted at constant impact angles of 45° to 90°. Eroded coatings surface roughness was found to follow target weight loss: The higher the weight loss, the higher the value of surface roughness observed. Erosion processes in the coatings were associated with formation of microcracks, microcrack propagation and intersection resulting in fragments of coatings which were then locally removed from the surface.

UNCLASSIFIED

SECURITY CLASSIFICATION OF THIS PAGE(When Data Entered)

PREFACE

This report summarizes research performed at the Israel Institute of Metals, Technion, Haifa, Israel from April 1980 through March 1981 under AFOSR Grant 80-0140. The work was initiated under Project 2422, "Protective Coatings and Materials", Task 2422 01, "Coatings for Aircraft and Spacecraft" and was funded under P.E. 62102F. The report was submitted in April 1981.

The author would like to acknowledge the support of Mr. George F. Schmitt, Jr., AFWAL/MLBE for assistance in writing the English version of this report and of Mr. Rod Darrah and Ms Janie Smith of Universal Energy Systems, Inc., Dayton, Ohio for preparation of the report and the figures therein.

Thanks are due to Mr. Shalom Feinberg, Israel Institute of Metals, Technion, Haifa for his valuable and efficient assistance.

Accession For	
NTIS GRA&I	<input checked="checked" type="checkbox"/>
DTIC TAB	<input type="checkbox"/>
Unannounced	<input type="checkbox"/>
Justification	
By	
Distribution/	
Availability Codes	
Dist	Avail and/or Special
A	

TABLE OF CONTENTS

	<u>Page</u>
1. Introduction.	1
2. Experimental Procedure.	2
3. Results	6
3.1 Erosion Kinetics.	6
3.1.1 Composite Materials.	6
3.1.2 Coatings	15
3.2 Surface Roughness	23
3.2.1 Coatings	23
3.3 Microscopic Observations.	30
3.3.1 Composite Materials.	30
3.3.2 Coatings	35
4. Discussion.	44
4.1 Composite Materials	44
4.1.1 Effect of Angle and Sand Weight Impacted	44
4.1.2 Surface Morphology	46
4.2 Coatings.	47
4.2.1 Effects of Angle and Sand Weight Impacted. . . .	47
4.2.2 Surface Roughness Effects.	51
4.2.3 Surface Morphology	52
5. Conclusions	54
5.1 Composite Materials - Conclusions	54
5.2 Coatings Materials - Conclusions	54
References	56
Appendix	
A. Erosion Weight Loss Data for Composites	58
B. Erosion Weight Loss Data for Coatings	63
C. Surface Roughness Data for Coatings	67

LIST OF ILLUSTRATIONS

<u>Figure</u>		<u>Page</u>
2.1	Schematic Drawing of the Air Blast Erosion Rig	4
3.1	Weight Loss of Quartz-Polyimide as a Function of Impact Angle.	8
3.2	Weight Loss of AFWAL/MLBE E-Glass Epoxy as a Function of Impact Angle.	9
3.3	Weight Loss of RAFAEL Glass Epoxy as a Function of Impact Angle	10
3.4	Weight Loss of Quartz-Polybutadiene as a Function of Impact Angle	11
3.5	Weight Loss as a Function of Sand Weight Impacted for Quartz-Polyimide	12
3.6	Weight Loss as a Function of Sand Weight Impacted for E Glass Epoxy.	13
3.7	Weight Loss as a Function of Sand Weight Impacted for Quartz-Polybutadiene	14
3.8	Weight Loss of MIL-C-8328 (Polyurethane on E Glass Epoxy as a Function of Impact Angle.	17
3.9	Weight Change of MIL-C-8323 (Polyurethane on E Glass Epoxy) as a Function of Impact Angle.	18
3.10	Weight Change of AF-C-VBW-15-15 Fluorocarbon on Quartz-Polyimide as a Function of Impact Angle.	19
3.11	Weight Loss of MIL-C-83786 Polyurethane/E Glass Epoxy as a Function of Sand Weight Impacted	20
3.12	Weight Change of MIL-C-83231 Polyurethane/E Glass Epoxy as a Function of Sand Weight Impacted.	21
3.13	Weight Change of AF-C-VBW-15-15 Fluorocarbon/Quartz Polyimide as a Function of Sand Weight Impacted	22
3.14	Surface Roughness of MIL-C-83286 Polyurethane as a Function of Impact Angle of Eroding Sand.	26
3.15	Surface Roughness of MIL-C-83231 Polyurethane as a Function of Impact Angle of Eroding Sand.	27
3.16	Surface Roughness of AF-C-VBW-15-15 Fluorocarbon as a Function of Impact Angle of Eroding Sand	28
3.17	Surface Profilograms for MIL-C-83231 Polyurethane.	29

<u>Figure</u>		<u>Page</u>
3.18	Uncoated Quartz-Polyimide Composite After 200 gr Sand Impact at 90° (30X)	32
3.19	Uncoated Quartz Polyimide and E Glass-Epoxy After 200 gr Sand Impacted at 90° (300X)	33
3.20	Uncoated Quartz-Polyimide and E Glass-Epoxy After 200 gr Sand Impacted at 90° (1500X)	33
3.21	Uncoated Glass-Epoxy (RAFAEL) After 200 gr Sand Impacted at 30° (30X and 1000X)	34
3.22	Uncoated Quartz-Polybutadiene After 200 gr Sand Impacted at 30° (500X and 500X)	34
3.23	MIL-C-83286 Polyurethane Coating on E Glass Epoxy Substrate After Sand Impact.	37
3.24	MIL-C-83286 Polyurethane Coatings on E Glass Epoxy Substrate After Sand Impact.	38
3.25	MIL-C-83231 Polyurethane Coating on E Glass Epoxy Substrate After Sand Impact.	39
3.26	MIL-C-83231 Polyurethane Coating on E Glass Epoxy Substrate After Sand Impact.	40
3.27	MIL-C-83231 Polyurethane Coating on E Glass Epoxy After 600 gr Sand Impacted at 90° (500 and 3000X)	40
3.28	AF-C-VBW-15-15 Fluorocarbon Coating on Quartz Polyimide Substrate After Sand Impact.	42
3.29	AF-C-VBW-15-15 Fluorocarbon Coating on Quartz Polyimide Substrate After 600 gr Sand Impacted at 90° (300X and 2000X)	43
4.1	Target Weight Changes as Function of Sand Weight Impacted at Constant Impact Angle of 30°	49
4.2	Target Weight Change as Function of Sand Weight Impacted at Constant Normal Impact Angle	50

LIST OF TABLES

<u>Table</u>		<u>Page</u>
A.1	Weight Loss Data for Quartz Polyimide Composite.	59
A.2	Weight Loss Data for AFWAL/MLBE E-Glass Epoxy.	60
A.3	Weight Loss Data for RAFAEL Glass Epoxy.	61
A.4	Weight Loss Data for Quartz-Polybutadiene.	62
B.1	Weight Loss Data for MIL-C-83286 Polyurethane on E Glass Epoxy.	64
B.2	Weight Loss Data for MIL-C-83231 Polyurethane on E Glass Epoxy.	65
B.3	Weight Loss Data for AF-C-VBW-15-15 Fluorocarbon on Quartz-Polyimide.	66
C.1	Surface Roughness Data for MIL-C-83286 Polyurethane/E Glass Epoxy.	68
C.2	Surface Roughness Data for Mil-C-83231 Polyurethane/E Glass Epoxy.	69
C.3	Surface Roughness Data for AF-C-VBW-15-15 Fluorocarbon/Quartz-Polyimide	70

1. Introduction

The erosion of polymeric coatings on composite materials by liquid impact in rain encounters of aircraft at moderate to high velocity has been a problem for many years.¹⁻³ The development of polyurethane and fluorocarbon elastomeric coatings for protection of forward facing reinforced plastic components such as radomes, antenna covers, jet engine fan blades, and helicopter rotor blades has been successful in achieving rain erosion protection of these materials.⁴ However, the erosion of these coatings and composite materials by solid particle impact has not been investigated since 1969.

Tilly⁵⁻⁷ has investigated the influence of velocity, impact angle, particle size, weight of abrasive (quartz particles) impacted, and type of reinforcement (glass versus carbon fiber) in plastic materials such as nylon polypropylene and epoxy resins. The composite materials exhibited poor erosion performance with the nylon exhibiting a four fold increase in erosion weight loss if reinforced with glass or carbon fibers and the epoxy showing a substantial improvement in erosion resistance if reinforced with steel powder compared to unreinforced material.

The purpose of this study was to determine the mechanisms of solid particle erosion on coatings which are representative of those currently used for exterior protection of aircraft surfaces--both reinforced composites and general skin surfaces, and on uncoated composite materials types (resins and fibers) and construction variables were determined.

2. Experimental Procedure

Apparatus

An air-blast sand erosion rig similar to that of Neilson and Gilchrist⁸ was used. Figure 2.1 shows the principal elements of the rig. Filtered compressed air at room temperature is partially by-passed through a sand reservoir from which the sand is picked up and introduced into the main stream through a control orifice. The air-sand stream then flows through a 4:1 converging nozzle into the specimen chamber.

The air flow rate was measured with an orifice flow meter. The actual mean velocity of the sand entering the specimen chamber was measured by the time-of-flight device suggested by Ruff and Ives.⁹ The device was inserted in place of the specimen chamber and calibrated against the normal air flow rate, which was subsequently used for control. In the air velocity range used, the sand velocity proved to be about one-third the air velocity, in agreement with the results of Ruff and Ives.

Target Materials

The test materials were as follows:

- A. Composite Materials. These were: Quartz polybutadiene and glass epoxy supplied by "RAFAEL" Armament Development Authority Haifa, Israel. Quartz-polyimide and E-Glass Epoxy supplied by AFWAL/MLBE Materials Laboratory, Wright-Patterson AFB, Ohio 45433, U.S.A.
- B. Coatings Materials. These were: MIL-C-83286 Polyurethane Topcoat on MIL-P-23377 Epoxy-Polyanide Primer. The substrate was E-Glass Epoxy as prepared. MIL-C-83231 Polyurethane Rain-Erosion-Resistant

Coating. The substrate was E-Glass Epoxy as prepared.

AF-C-VBW-15-15 fluorocarbon-rain-erosion-resistant-coating.

The substrate was Quartz-Polyimide as prepared. All the coatings were supplied by AFWAL/MLBE Materials Laboratory, Wright Patterson AFB, Ohio 45433, U.S.A. Specimen of composite and coating materials were cut to measures of 50 mm by 60 mm.

Sand

Natural sand collected from the shore of the Mediterranean Sea was sieved into the range of 210 to 297 μm and oven dried. This sand contained about 96 percent by weight of SiO_2 , the constituent considered to be responsible for its erosiveness.¹⁰ The grains were slightly rounded and somewhat elongated.

Erosion Tests

The sand reservoir was filled with sand in amounts varying between 50 and 600 gr and the experimental run continued until all the sand had been exhausted from the reservoir. The maximum air velocity used was 150 m/sec. and the specimen impact angles were 90° , 75° , 60° , 45° , 30° and 15° . Three to five runs were made for each experimental condition of air velocity, impingement angle, sand quantity and target. Before and after exposure the specimens were weighed to 0.1 mg on an analytical balance.

Surface Characterization

Electron Microscopy. The surfaces of the specimens were examined directly with a scanning electron microscope together with an X-ray

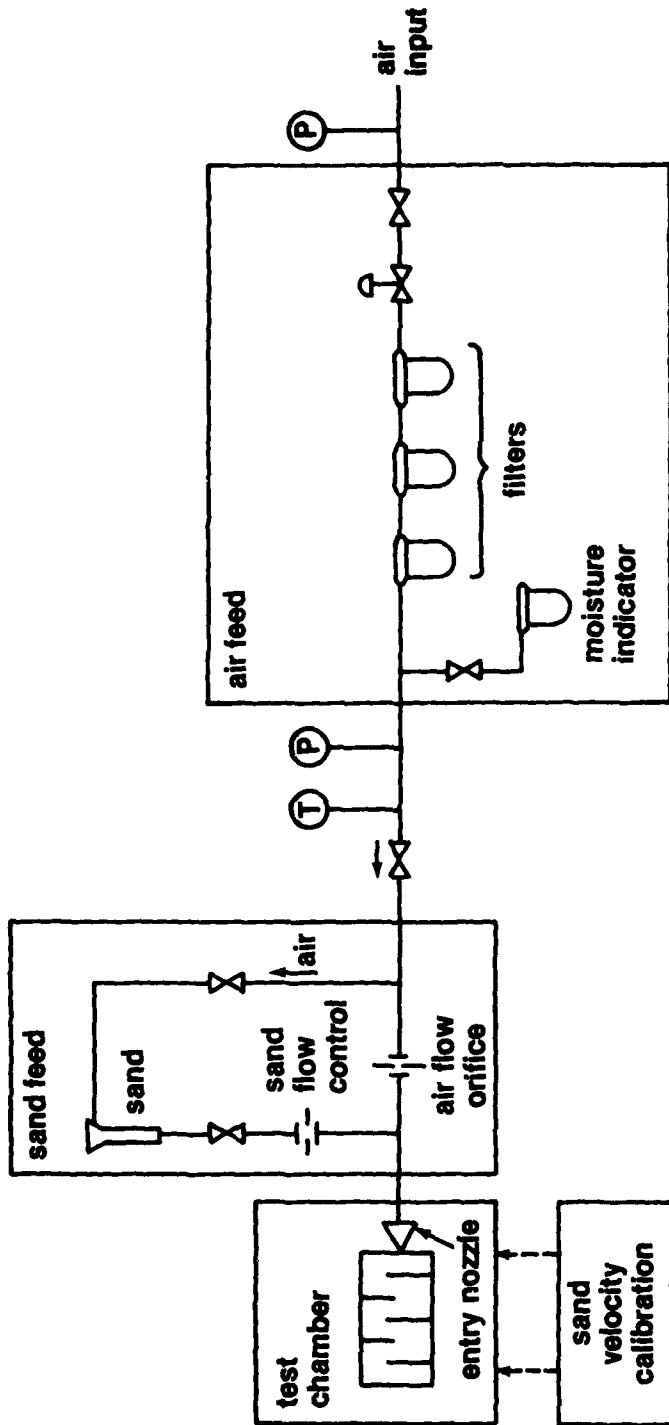


Fig. 2.1 Schematic Drawing of the Air Blast Erosion Rig

unit. Cross section of eroded specimens were also examined with the electron probe microanalyzer (EPM).

Roughness Measurement. The roughness of the target specimens was measured before and after erosion with a Talysurf, Hobson Model 3. Graphs of the Surface Profile were obtained. The roughness is expressed as the centerline average (CLA).¹¹

3. Results

The materials investigated were classified into two major groups:

- A. Composite materials which included Quartz/polyimide, E-Glass Epoxy and Quartz/polybutadiene laminates.
- B. Coatings materials such as polyurethane (2 types) and fluorocarbon on Glass/Epoxy and Quartz/Polyimide substrates respectively.

Specimens were exposed to sand erosion conditions of natural sand abrasive particles, 210 to 297 microns in size with amounts impacted from 200 gr to 600 gr at impact angles of 15° to 90° and impact velocity up to 0.1 Mach.

Weight change, surface roughness and surface morphology were examined and correlated with erosion conditions, primarily, impact angles and mass of sand impacted. The results are described in the following sections.

3.1 Erosion Kinetics

3.1.1 Composite Materials

Erosion data, namely target weight change obtained under various sand erosion conditions, is summarized in Appendix A, Tables A.1 to A.4, and shown graphically in Figures 3.1 to 3.7.

A. Target Weight Change vs. Impact Angle

The effect of impact angles on target weight under constant amount of sand impacted is shown graphically in Figures 3.1 to 3.4. A progressive increase in target weight loss was observed with increasing

impact angle up to 75° where a maximum weight loss was found in Quartz polyimide (Figure 3.1), Glass Epoxy (Figure 3.3), and Quartz Polybutadiene (Figure 3.4). This behavior was observed with constant amounts of 200 gr, 400 gr, and 600 gr of abrasive sand. Particles impacted on the target surface resulted in weight loss in the range of hundreds of milligrams up to 500 mg. (Figures 3.1, 3.3, 3.4). The behavior of E-Glass Epoxy material (AFWAL/MLBE) under the same erosion conditions used with the above composite materials is shown in Figure 3.2. Increase in impact angle resulted in increased target weight loss up to a maximum at 60° , 45° and 45° for impacted sand amounts of 200 gr, 400 gr, and 600 gr, respectively (Figure 3.2). After reaching a maximum, target weight loss decreased to a minimum at normal impact angle. Furthermore, in the case of E-Glass/Epoxy (AFWAL/MLBE), the weight loss was in the range of tens of milligrams compared to hundreds found in the other composite materials.

B. Target Weight Changes vs. Sand Weight Impacted

The dependence of target weight change on amounts of sand impacted under constant impact angles for the composite material is described in Figures 3.5, 3.6 and 3.7. It was found that an increase in the amount of sand weight impacted resulted in progressive target weight losses under all impact angles investigated as can be seen in Figure 3.5 for Quartz Polyimide, Figure 3.6 for E Glass-Epoxy (AFWAL/MLBE) and Figure 3.7 for Quartz Polybutadiene and Glass/Epoxy (RAFAEL). Although the E Glass/Epoxy (AFWAL/MLBE) materials behaved similarly to the other materials under the same erosion condition, the amounts of

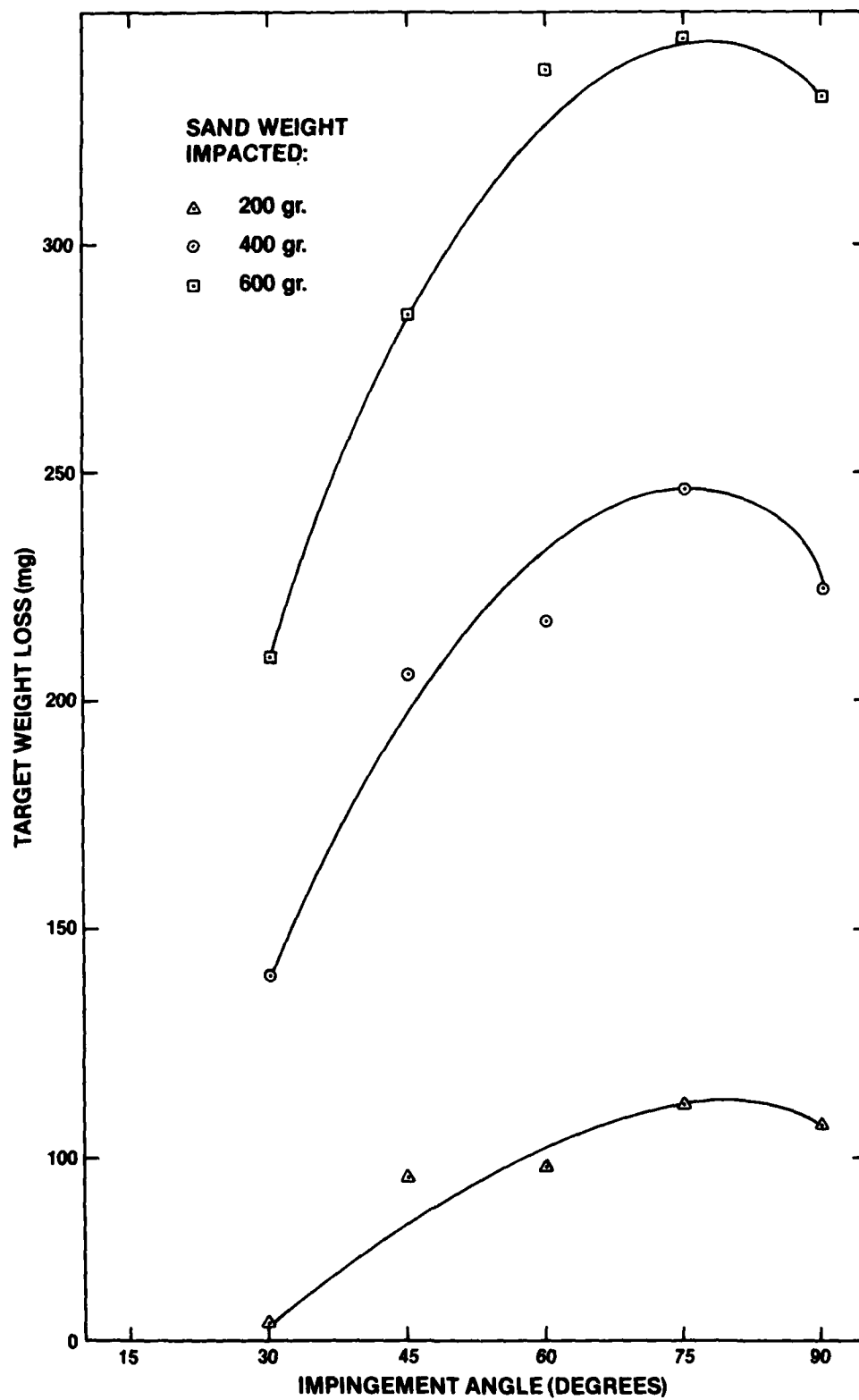


Fig. 3.1 Weight Loss of Quartz-Polyimide as a Function of Impact Angle

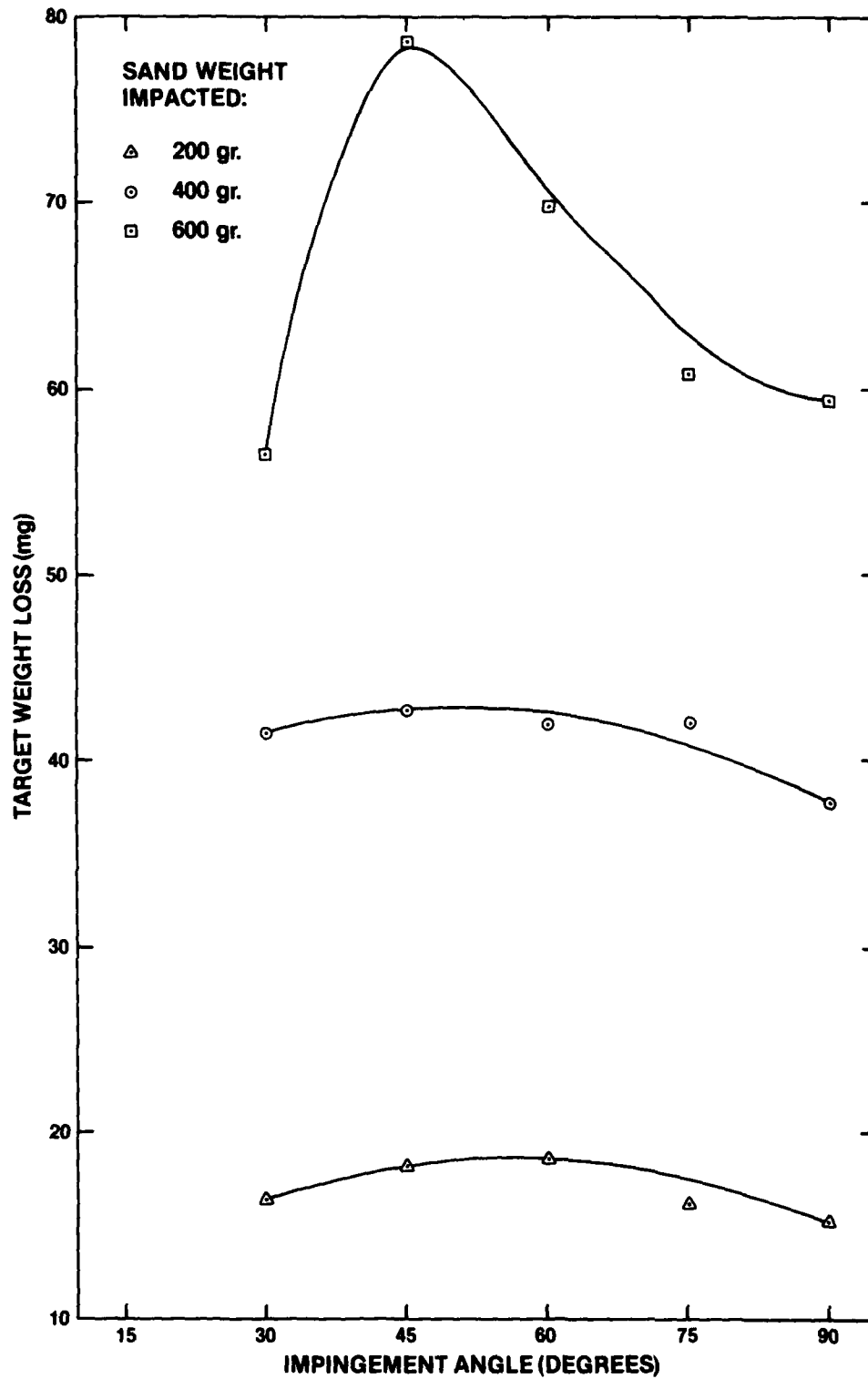


Fig. 3.2 Weight Loss of AFWAL/MLBE E-Glass Epoxy as a Function of Impact Angle

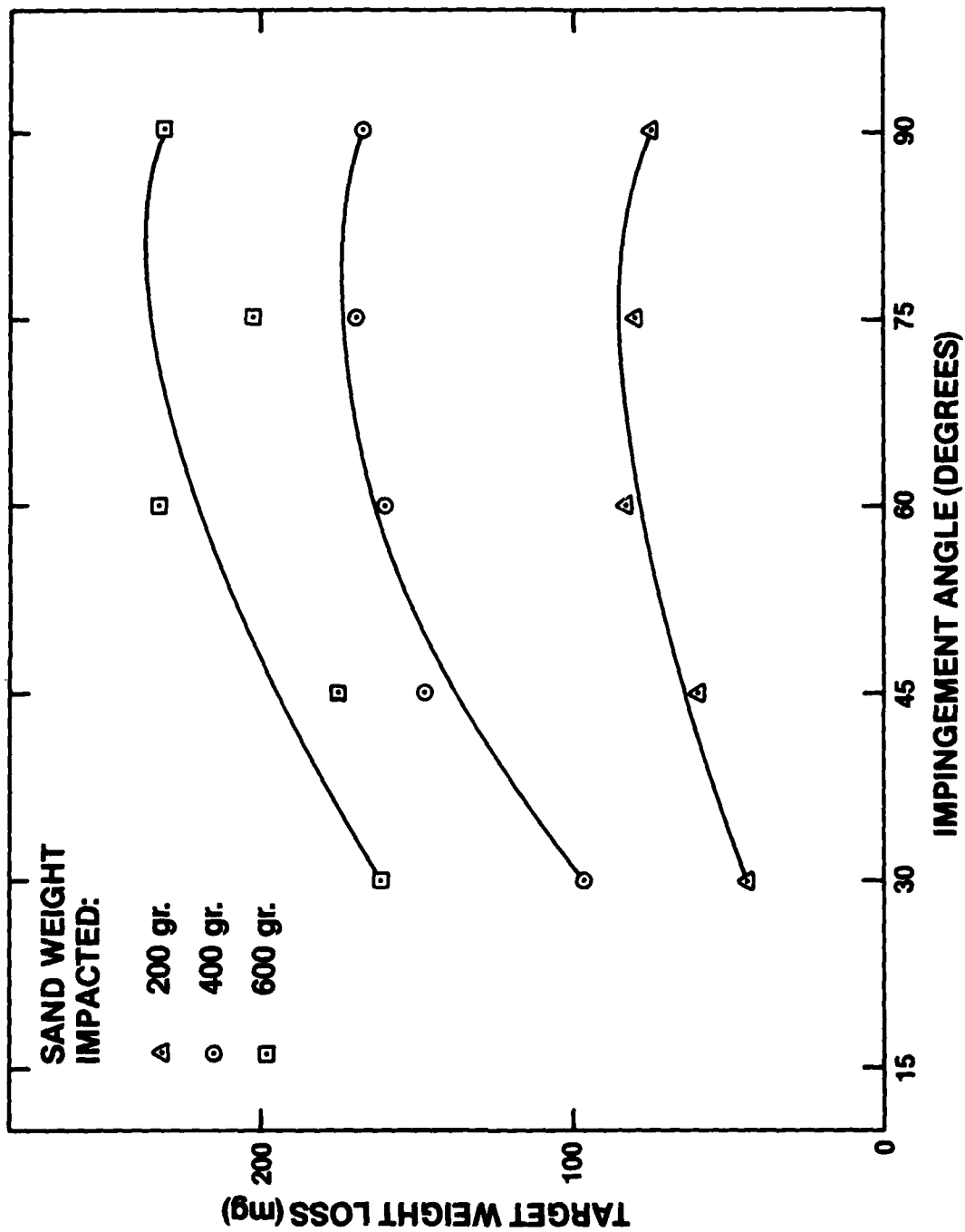


Fig. 3.3 Weight Loss of RAFAEL Glass Epoxy as a Function of Impact Angle

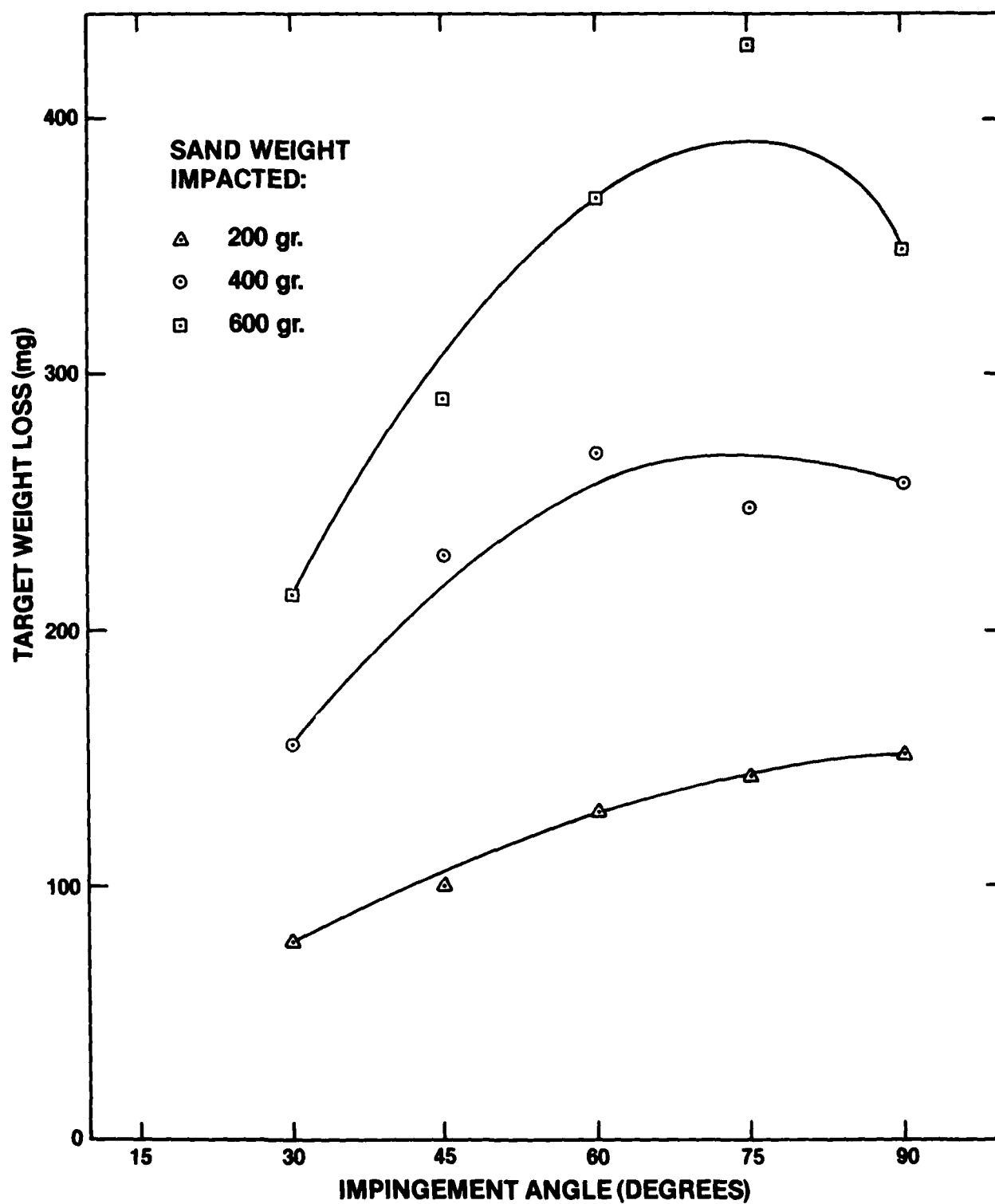


Fig. 3.4 Weight Loss of Quartz-Polybutadiene as a Function of Impact Angle

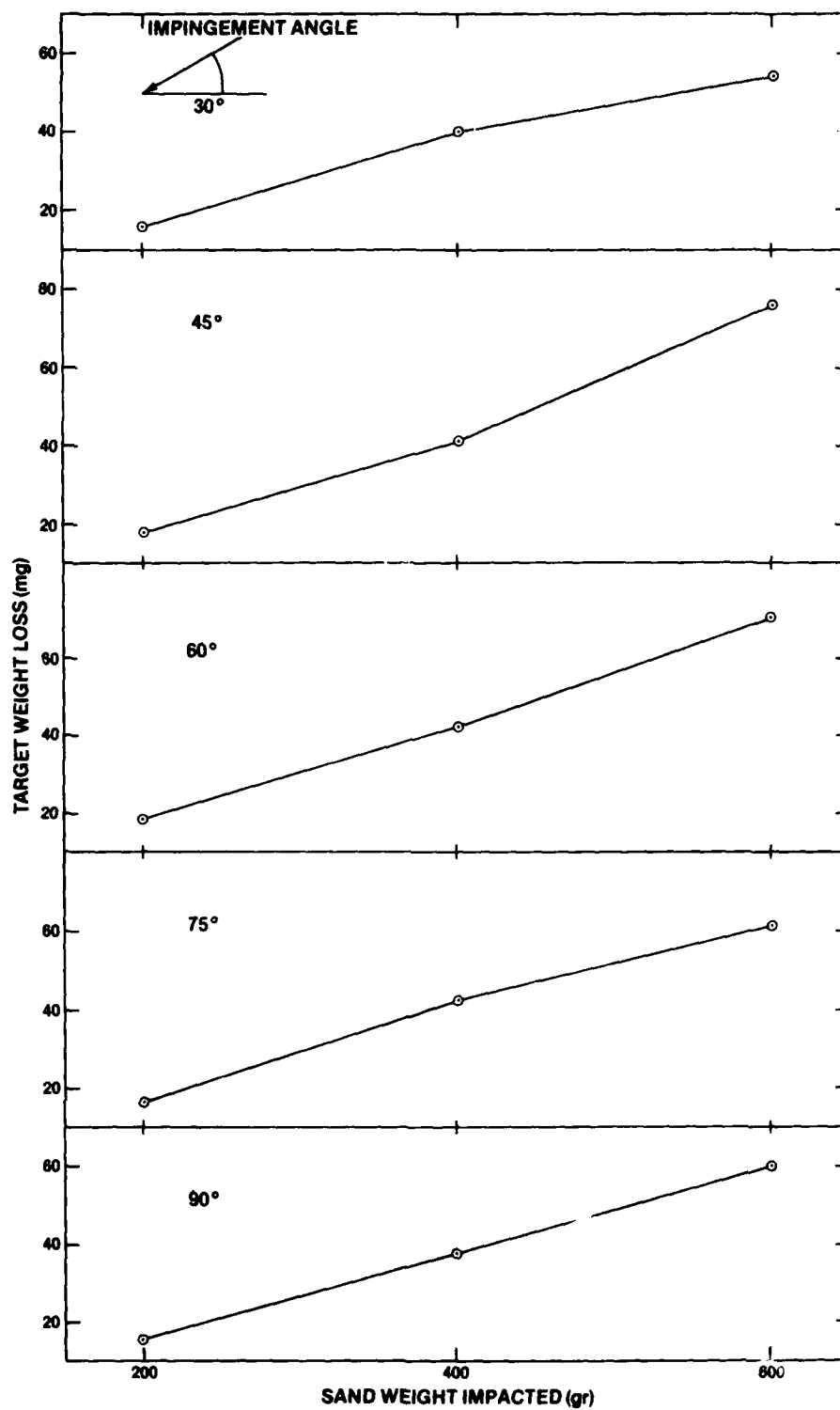


Fig. 3.5 Weight Loss as a Function of Sand Weight Impacted for Quartz-Polyimide

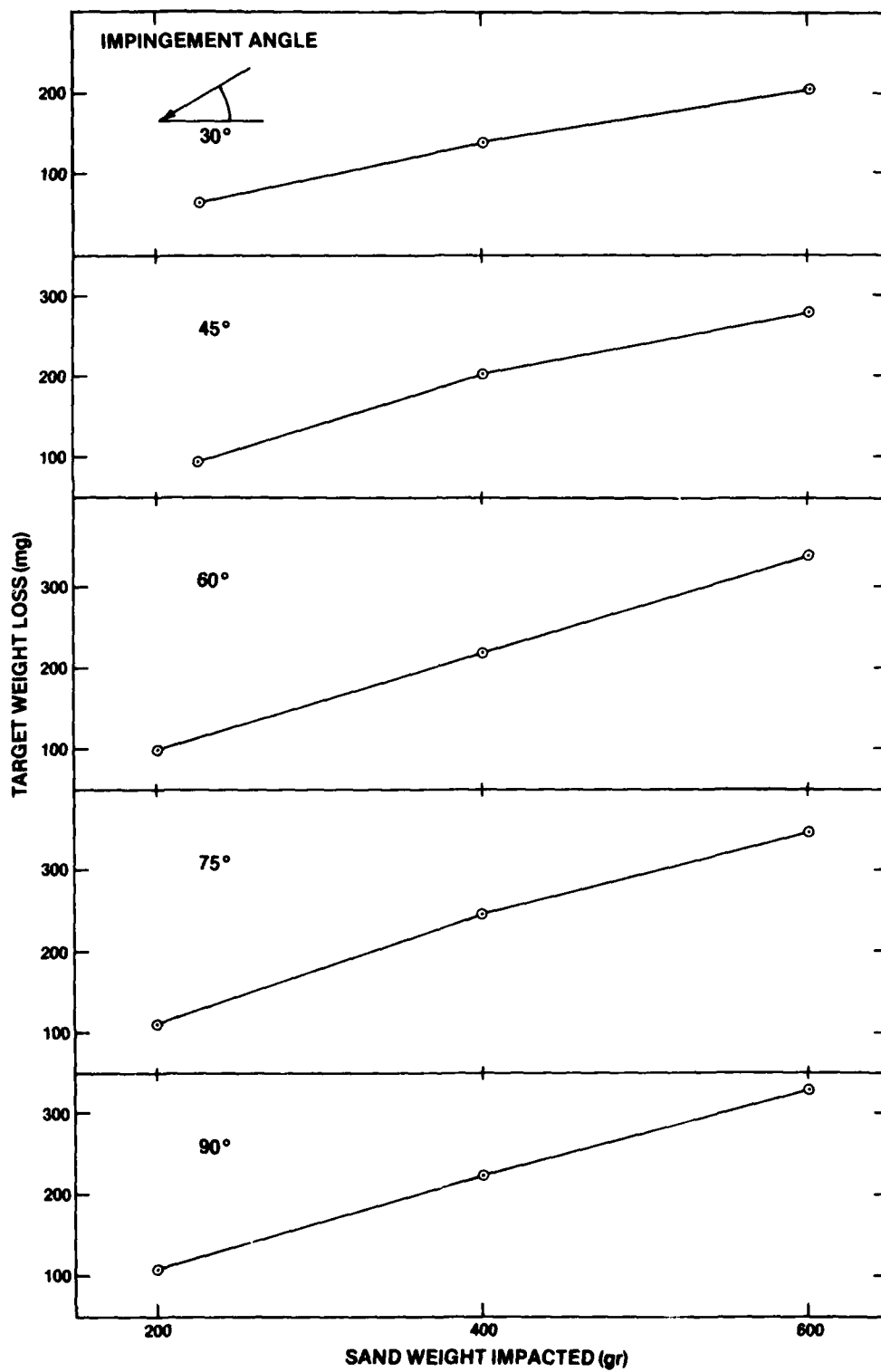


Fig. 3.6 Weight Loss as a Function of Sand Weight Impacted for E Glass Epoxy

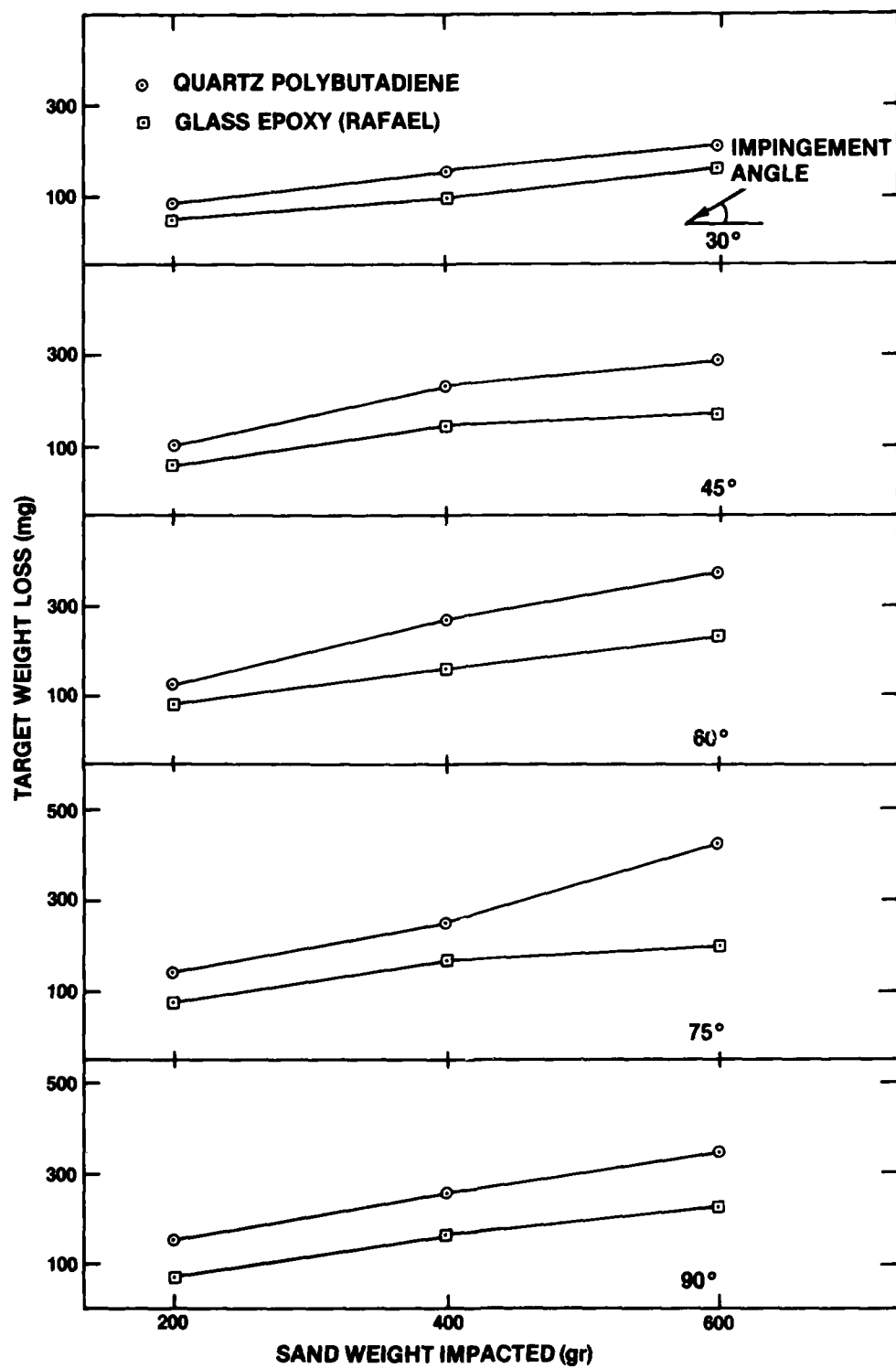


Fig. 3.7 Weight Loss as Function of Sand Weight Impacted for Quartz-Polybutadiene

target weight losses for it were found to be in the range of 80 mg. (Figure 3.6) compared to the range of 500 mg; that is, an order of magnitude lower than the others (Figure 3.5 for Quartz-polyimide and 3.7 for Glass Epoxy (RAFAEL) and Quartz polybutadiene). Furthermore, it was found that the increase of target weight loss with increase of sand weight impacted took place at low as well as high impact angles.

3.1.2 Coatings

Exposure of polyurethane and fluorocarbon coatings to various sand erosion conditions resulted in erosive damage to the coatings surface. The experimental data is summarized in Appendix B, Tables B.1, B.2, and B.3. The results are characterized in terms of target weight change versus impact angles and total sand weight impacted as will be described herein.

A. Target Weight Change vs. Impact Angles

The dependence of coating target weight change on impingement angles before and after being exposed to sand erosion conditions is shown graphically in Figures 3.8, 3.9 and 3.10 as well as in Appendix B, Tables B.1-B.3. Figure 3.8 shows the behavior of MIL-C-83286 polyurethane coatings on E Glass Epoxy substrate under the impact of 200, 400, and 600 gr abrasive and particles on the target surface. A correlation between target weight loss and impingement angle was found (Figure 3.8). Maximum weight loss was found at low impact angle resulted in decreasing target weight loss which was around 80% for normal impact angle and all the amounts of sand particles weight impacted (Figure 3.8). The

behavior of MIC-C-83231 polyurethane coating on E-Glass Epoxy substrate under erosion conditions is shown in Figure 3.9. It was found that under constant amount of sand particles impacted (200, 400, 600 gr, respectively), a maximum target weight loss was obtained at low incidence angle of 15° . Increasing the impact angle up to 45° resulted in reduced target weight loss. Furthermore, at impact angles of 45° and higher, target weight gain was found to be constant and practically independent of the impact angle (See Figure 3.9).

In Figure 3.10 the behavior of AF-C-VBW-15-15 fluorocarbon coatings on quartz polyimide under erosive conditions is shown. Target weight change as a function of impingement angle was obtained under constant amounts of 200 gr, 400 gr, and 600 gr of sand particles impacted. Maximum target weight loss was obtained at impact angle 30° ; whereas at around 50° a zero weight loss was observed. Increasing the impact angle from 50° up to 90° led to target weight gain as can be seen in Figure 3.10.

B. Coatings Target Weight Change vs. Sand Weight Impacted

A correlation between weight change of polyurethane coating on E Glass Epoxy substrate (AFWAL/MLBE) and the amount of sand particles impacted at constant impingement angles is shown in Figure 3.11 and 3.12 for MIL-C-83286 polyurethane and MIL-C-83231 polyurethane, respectively. Figure 3.12 shows that increasing the amount of sand weight impacted in the range of 200 to 600 gr resulted in an increase of target weight loss for the hard polyurethane. Moreover, the rate (i.e., the amount of target weight loss to amount of sand impacted) decreased from

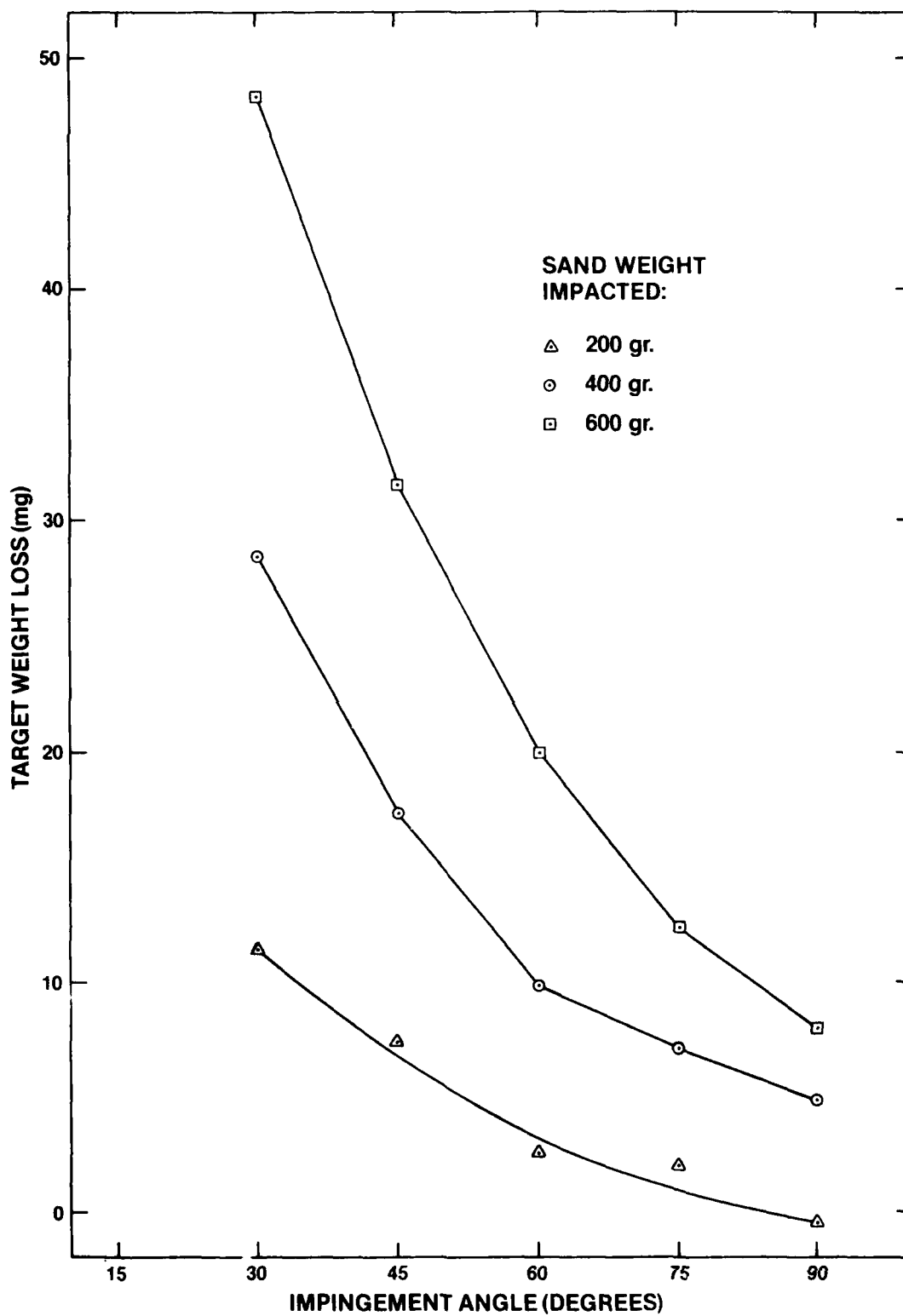


Fig. 3.8 Weight Loss of MIL-C-83286 Polyurethane E Glass-Epoxy as a Function of Impact Angle

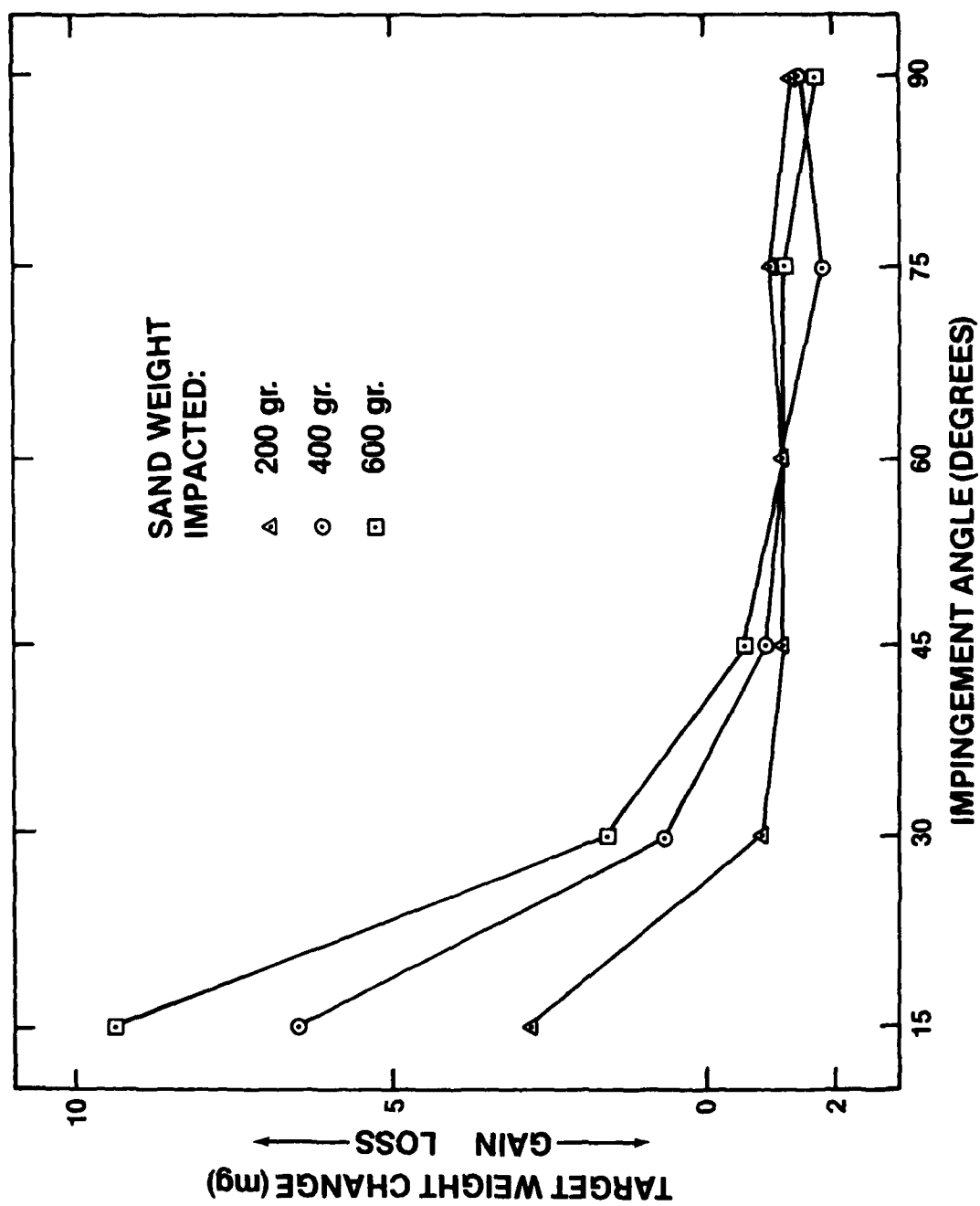


Fig. 3.9 Weight Change of MIL-C-8323 1 Polyurethane on E Glass-Epoxy as a Function of Impact Angle

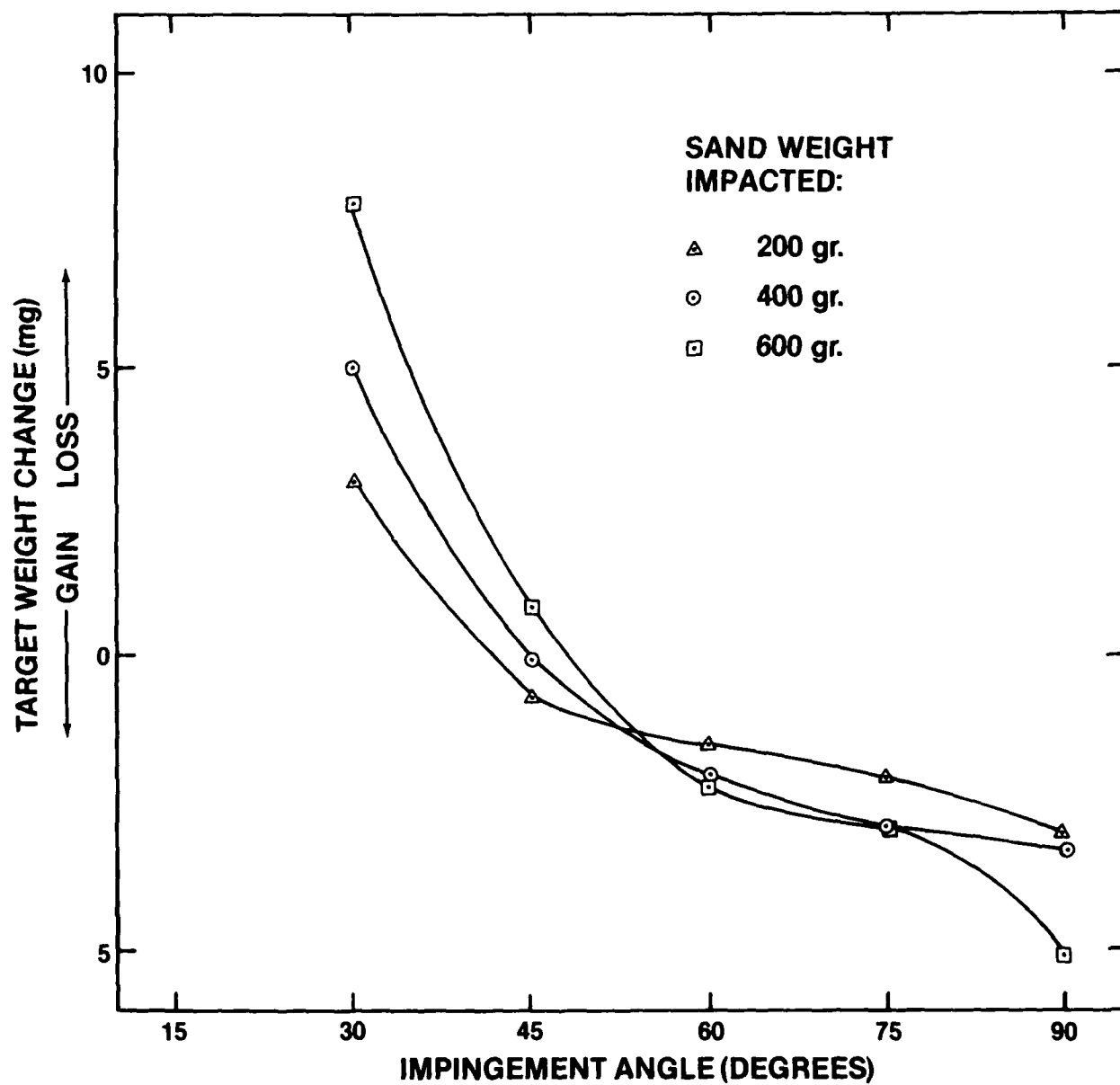


Fig. 3.10 Weight Change of AF-C-VBW-15-15 Fluorocarbon on Quartz-Polyimide as a Function of Impact Angle

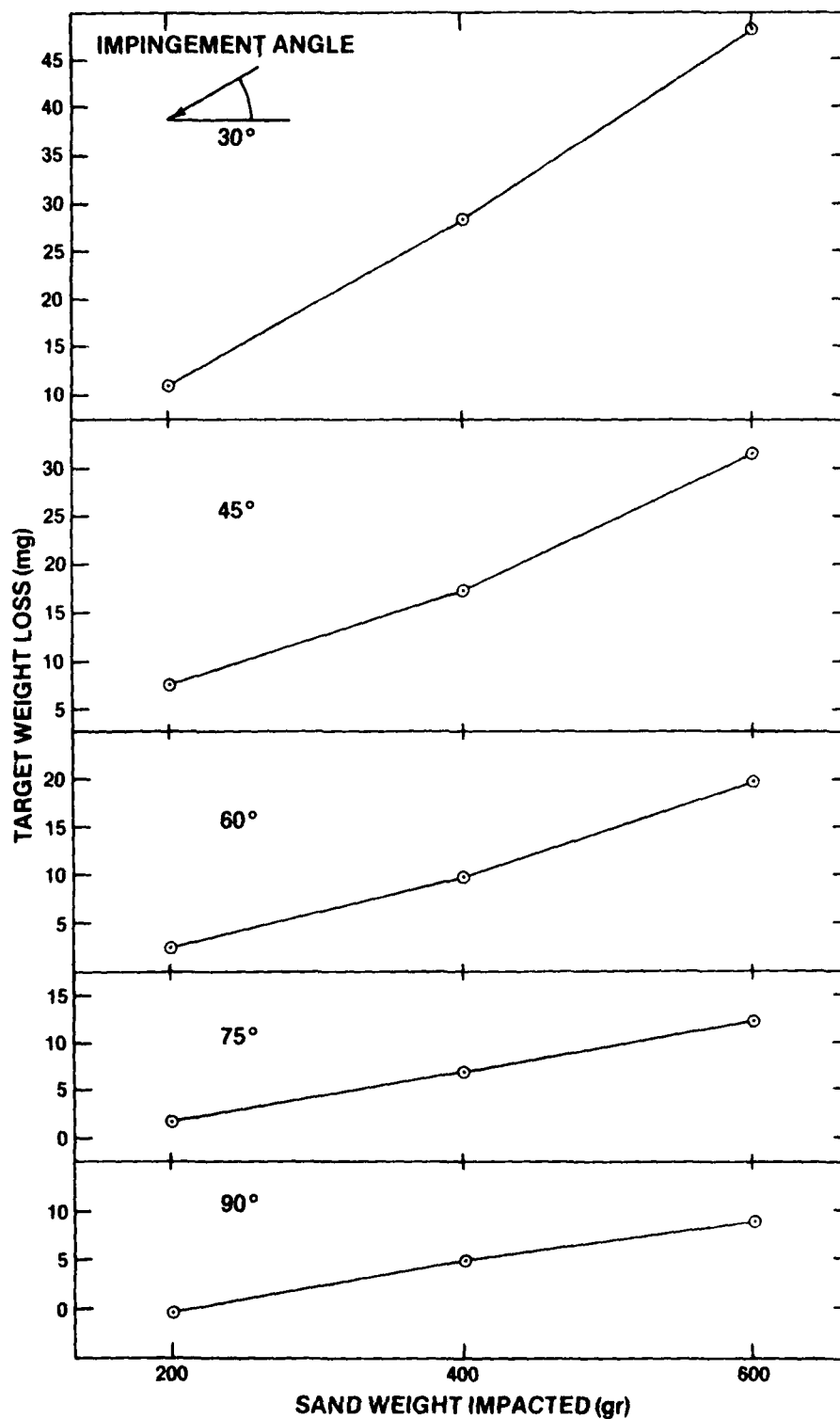


Fig. 3.11 Weight Loss of MIL-C-83286 Polyurethane/E Glass Epoxy as a Function of Sand Weight Impacted

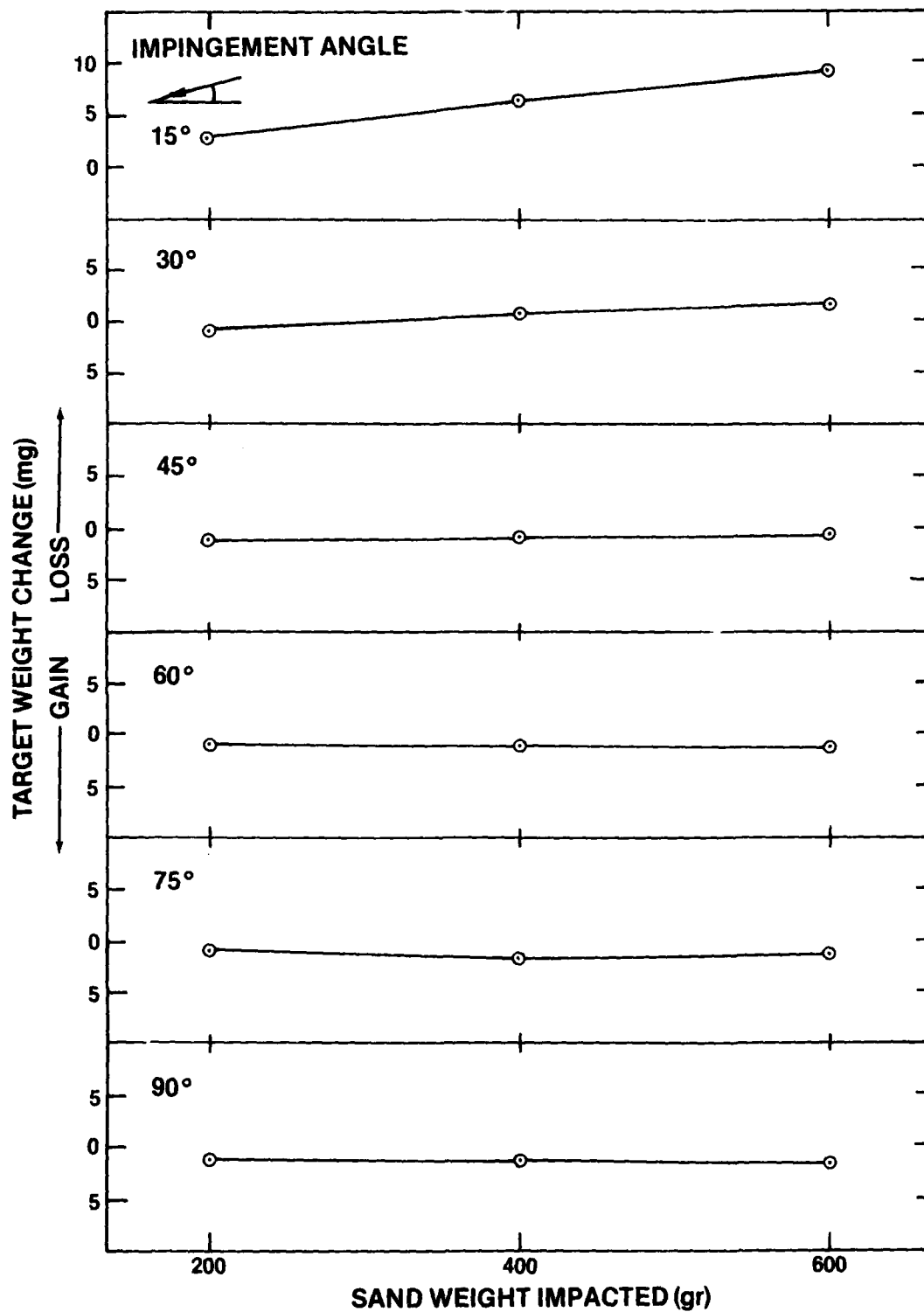


Fig. 3.12 Weight Change of MIL-C-83231 Polyurethane/E Glass Epoxy as a Function of Sand Weight Impacted

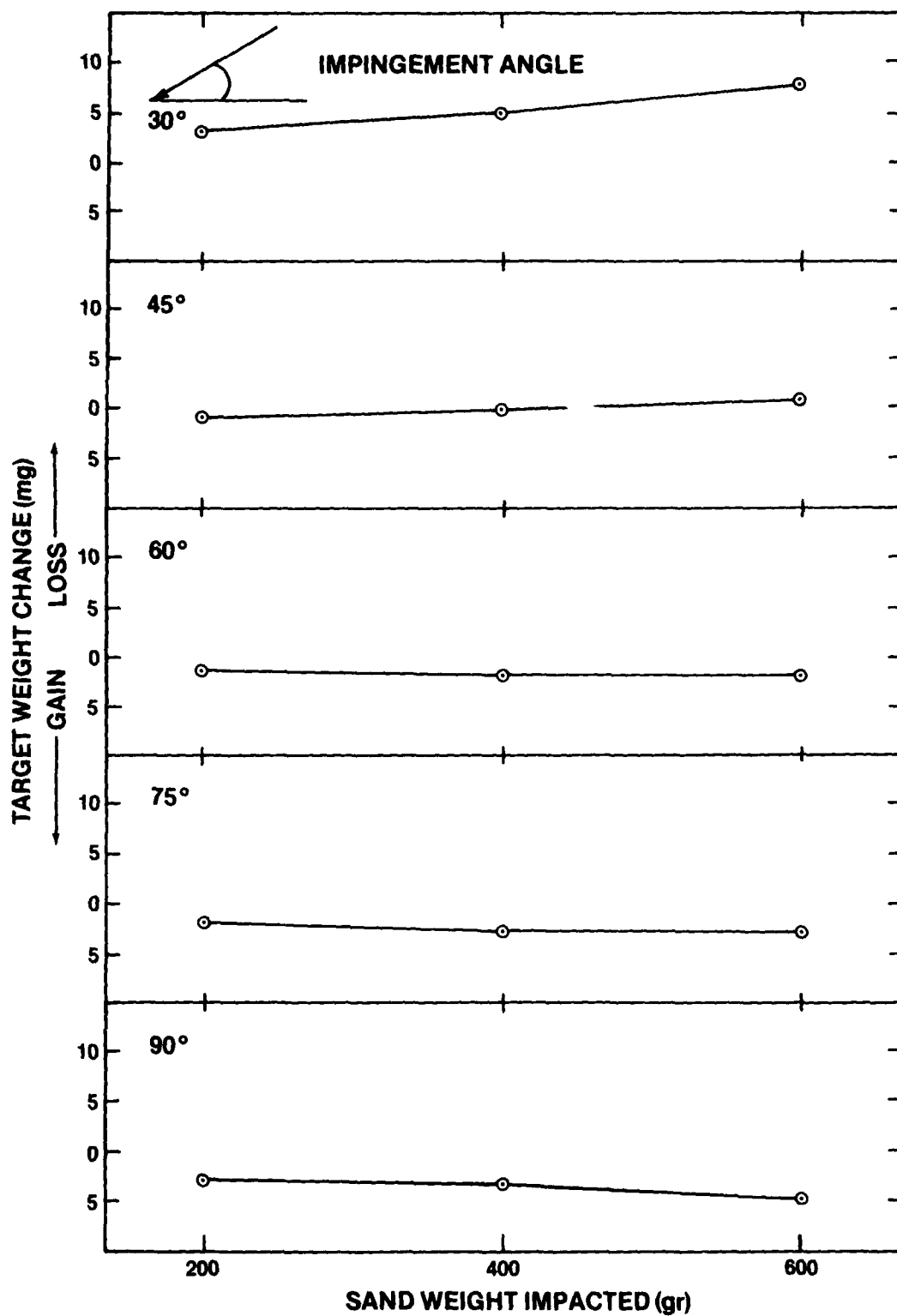


Fig. 3.13 Weight Change of AF-C-VBW-15-15 Fluorocarbon/
Quartz Polyimide as a Function of Sand Weight
Impacted

a maximum value at impact angle of 30° to a minimum at 90° (Figure 3.11).

Coating weight loss at 30° was 36.9 gr compared to 9.5 gr at 90° at the same amount of 400 gr sand impacted.

The MIL-C-83231 elastomeric polyurethane coating was found to behave differently compared to the MIL-C-83286 polyurethane under the same erosion condition. As shown in Figure 3.12, weight changes of MIL-C-83231 polyurethane coatings were found to be independent of the amount of sand impacted (200 gr to 600 gr) under impact angles of 45° to 90° . At lower impact angles of 30° to 45° a linear increase of target weight loss was found. Moreover, increasing weight gain rather than loss was found in this coating when increasing the amount of sand impacted at constant impact angles of 45° to 90° .

The behavior of AF-C-VBW-15-15 fluorocarbon coatings on Quartz polyimide substrate was found to be very similar to the MIL-C-83231 polyurethane coating under the same erosion conditions as can be seen in Figure 3.13.

A continuously increasing weight gain of fluorocarbon coatings was found after being exposed to various amount of sand particles (200 gr to 600 gr) at constant impact angles of 45° to 90° . When the impact angle was 30° , a linear correlation between target weight loss and amount of sand impacted was found (Figure 3.13).

3.2 Surface Roughness

3.2.1 Coatings

The characterization of eroded coatings surface included measurements of surface roughness. The data obtained is summarized in

Appendix C. Tables C.1, C.2 and C.3 are shown graphically in Figure 3.14, 3.15 and 3.16, respectively.

MIL-C-83286 Polyurethane Coatings. A dependence of target surface roughness expressed in C.L.A. (centre line average) in microns on impingement angle for constant amounts of sand impacted is shown in Figure 3.14. The results show that high surface roughness C.L.A. around 2.2 microns was obtained at impingement angles of 30° to 45° for all amounts (200, 400, and 600 gr) of sand impacted. Increasing the impact angles up to 90° led to a sharp decrease in surface roughness reaching values around 1.4 microns at 90° .

MIL-C-83231 Polyurethane Coatings. The change of coatings surface roughness with impact angle at various constant amounts of sand impacted are shown in Figure 3.15. Surface roughness was found to decrease from a maximum in the range of 0.4 to 1.0 micron at impact angles of 15° to a constant low values around 0.2 microns at impact angles of 60° to 90° . A profilogram of the surface before and after being exposed to erosion is shown in Figure 3.17.

A rather smooth profile was obtained before erosion, whereas after being exposed to 200 gr and 400 gr sand particles at 10° , a rough profile was obtained with about 5 microns peak to peak and average peak width of 25 microns (Figure 3.17). Increasing the impact angle, led to a smoother surface with lowest profile at 90° . The profilograms exhibited high surface roughness at low incident angle compared to low surface roughness at normal angles.

AF-C-VBW-15-15 Fluorocarbon Coatings. Surface roughness of this coating is correlated versus impingement angles for constant amounts of 200 gr, 400 gr, and 600 gr sand particles impacted. The correlation is shown in Figure 3.16. Maximum surface roughness in the range of 1.0 to 1.6 microns was found at impact angle of 30° for all amounts of sand impacted. A decrease in surface roughness was found with increasing impact angle. A constant low surface roughness value around 0.8 micron was found at impact angles from 45° to 90° (Figure 3.16). It should be noted that the low value of surface roughness of the polyurethane coating was around 0.2 microns compared to 0.8 microns in the fluorocarbon coatings.

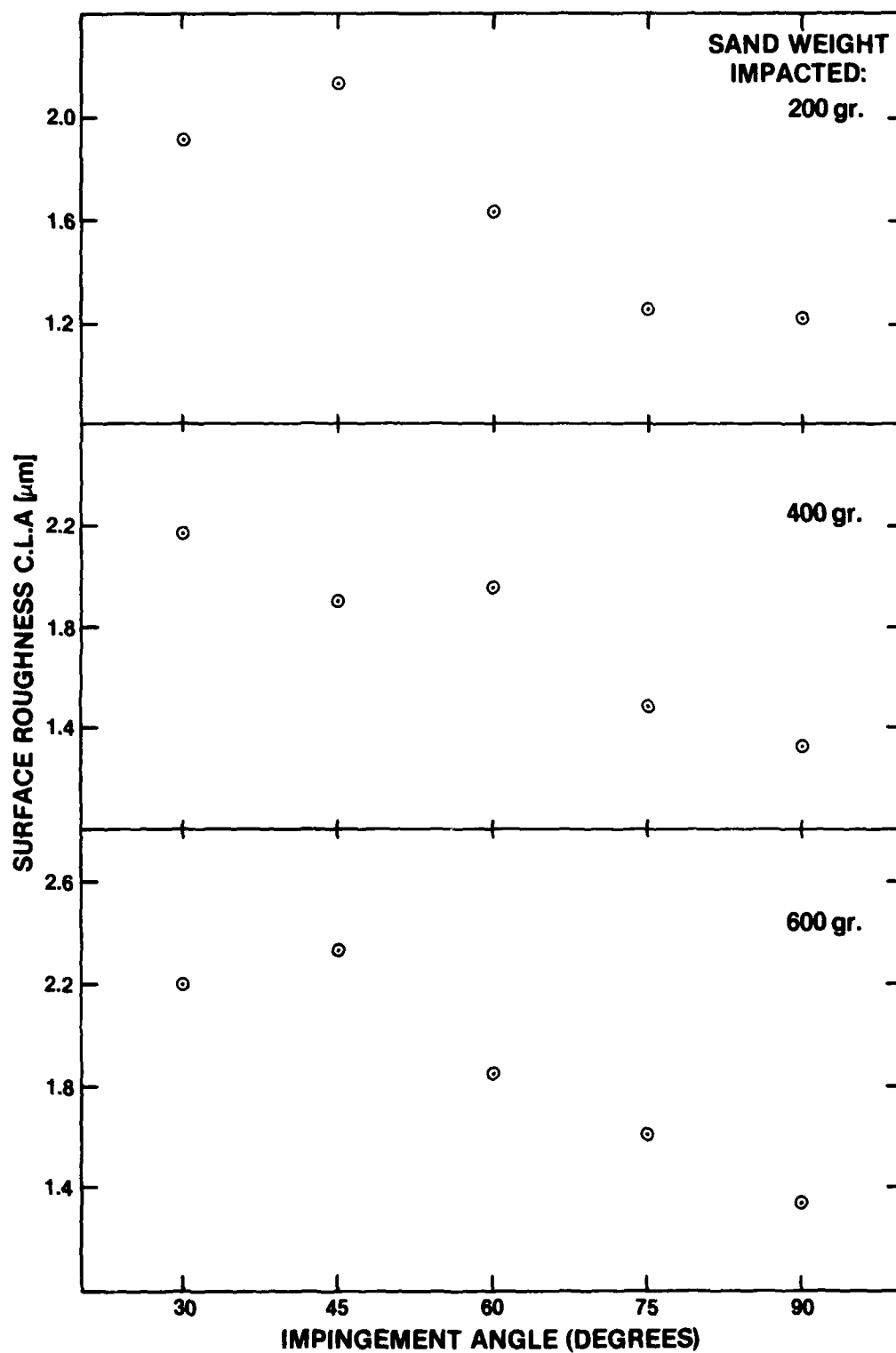


Fig. 3.14 Surface Roughness of MIL-C-83286 Polyurethane as a Function of Impact Angle of Eroding Sand

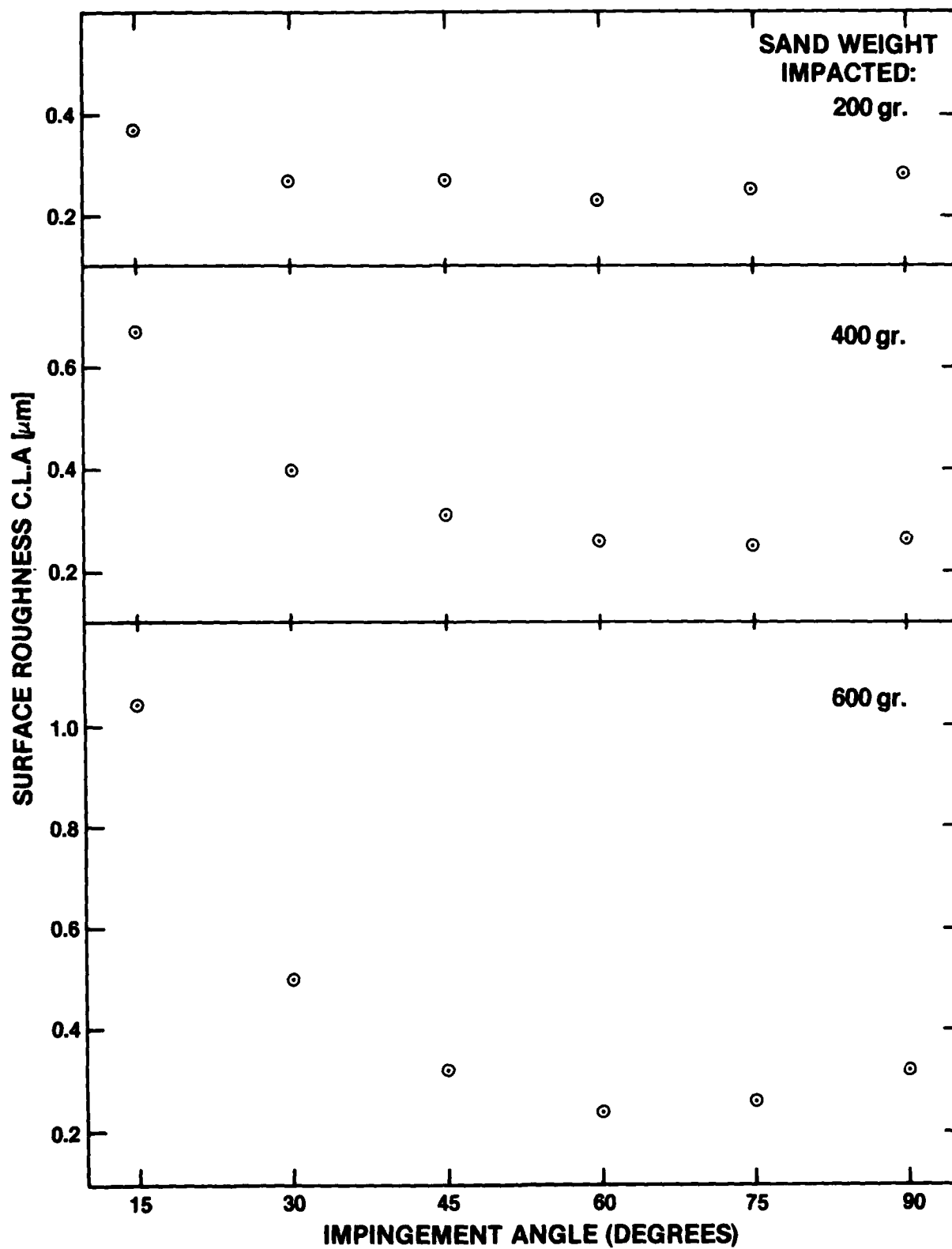


Fig. 3.15 Surface Roughness of MIL-C-83231 Polyurethane as a Function of Impact Angle of Eroding Sand

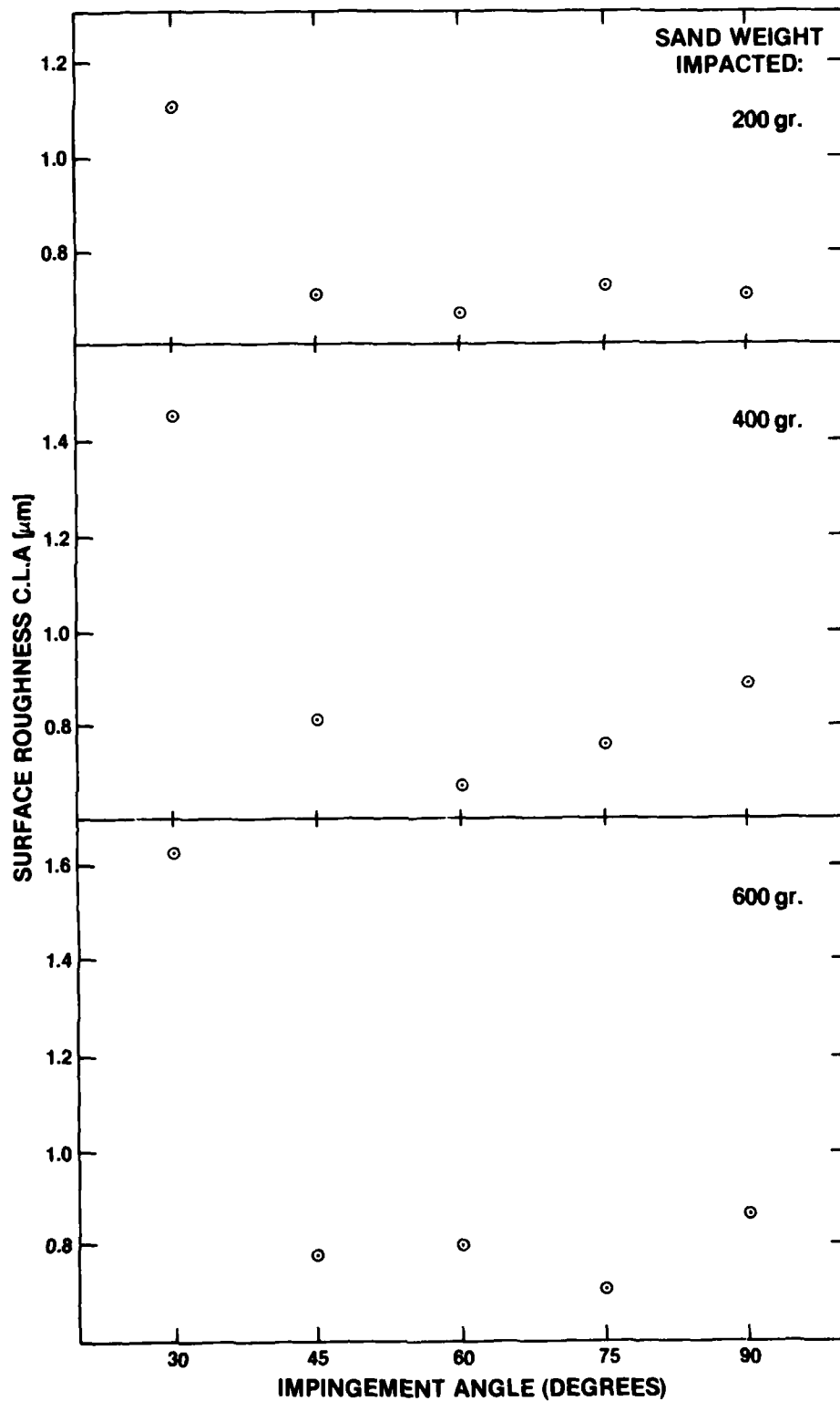


Fig. 3.16 Surface Roughness of AF-C-VBW-15-15 Fluorocarbon as a Function of Impact Angle of Eroding Sand

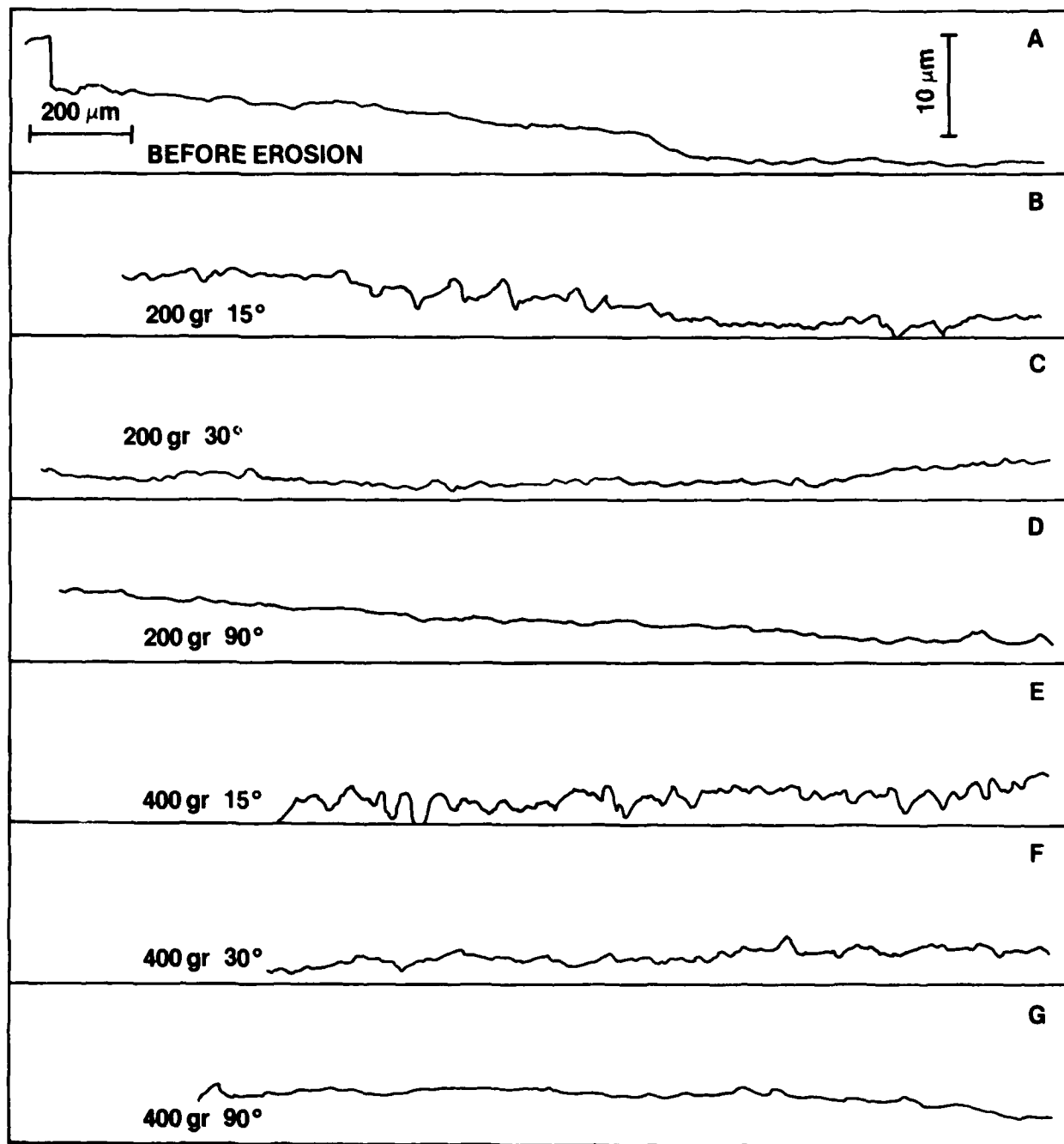


Fig. 3.17 Surface Profilograms for MIL-C-83231 Polyurethane

3.3 Microscopic Observations

3.3.1 Composite Materials

Eroded surfaces of various target composites investigated in the research work were examined by scanning electron microscope and the results are shown in Figures 3.18 to 3.22. A typical eroded surface of quartz-polyimide composite material is shown at low magnification in Figure 3.18. The cross junctions of the quartz weaves as well as the polyimide resin zones are shown very clearly. Moreover, the erosion damage was observed both in the fibers as well as in the resin zones.

A detailed picture of the damage caused by the erosion processes in the fibers zones can be seen clearly in Figures 3.19 and 3.20 for quartz polyimide and Glass Epoxy composites.

The erosion damage observed was characterized by broken fibers (Figure 3.19) and detachment of fibers from the resin matrix (Figure 3.20) which resulted in removal of fiber fragments from the eroded areas. These fragments of fibers are about 10 microns in width and about 30 microns in length. Also smaller fragments could be observed both in the E Glass Epoxy and Quartz polyimide targets which each showed similar erosion damage. In Figure 3.21 SEM micrographs of other eroded Glass Epoxy (RAFAEL) composite are shown at low (Figure 3.21A) and high (Figure 3.22A) magnification. Erosion damage was observed both in the glass fiber areas as well as in the epoxy resin zone (Figure 3.21A, 200 gr sand, 30°). High magnification image of the eroded surface revealed broken glass fibers, fragments of fibers as well as craters in the epoxy resin zone indicative of local material removal from that zone (See Figure 3.21B). Furthermore,

removal of the epoxy resin material by the erosion process revealed previously unexposed glass fibers which would then be subjected to the erosion process as shown in Figure 3.21B. A typical erosion damage observed in quartz polybutadiene after being exposed to 200 gr sand at 30^0 is shown in Figure 3.22. The morphology of the eroded surface in the polybutadiene resin zone is shown in Figure 3.22A.

Craters and grooves of 30 μm size were observed in the surface indicative of local material removal by erosion process (Figure 3.22A). In the quartz fiber zone, the erosion damage was characterized by broken fibers, removal of fibers fragments which were approximately 10 microns in width and 30 microns in length as shown in Figure 3.22B.

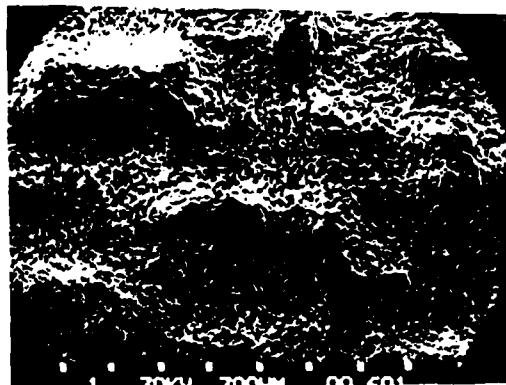
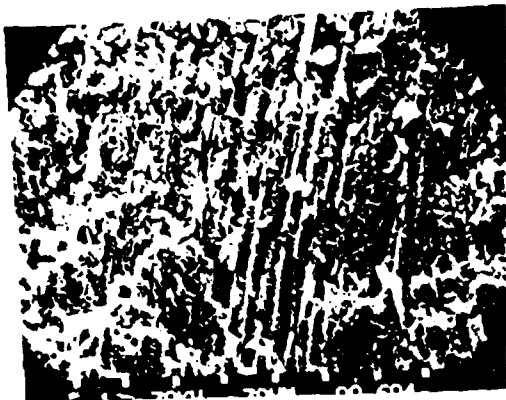


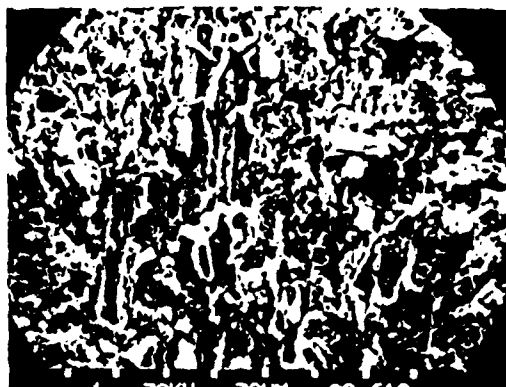
Fig. 3.18

Uncoated Quartz-Polyimide Composite after 200 g.
Sand Impact at 90° (30X)

SEM Micrograph



A



B

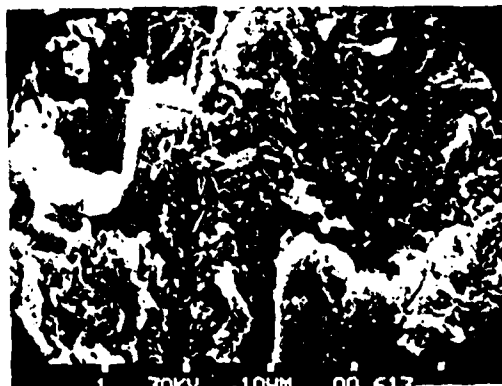
Fig. 3.19 Uncoated Quartz Polyimide and E Glass-Epoxy after
200g Sand Impacted at 90° (300X)
SEM Micrograph

A. Quartz Polyimide

B. E Glass-Epoxy



A



B

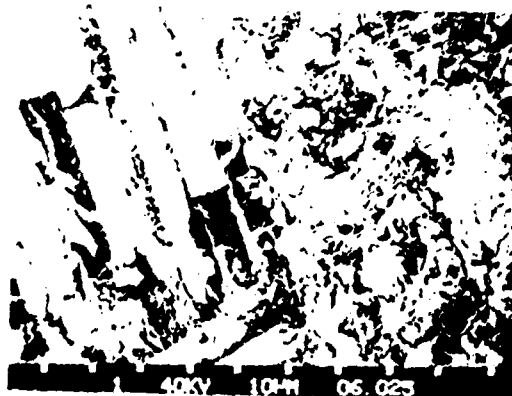
Fig. 3.20 Uncoated Quartz-Polyimide and E Glass-Epoxy after
200g Sand Impacted at 90° (1500X)
SEM Micrograph

A. Quartz Polyimide

B. E Glass-Epoxy



A

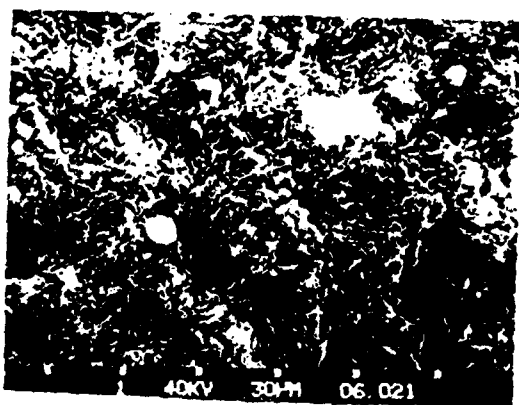


B

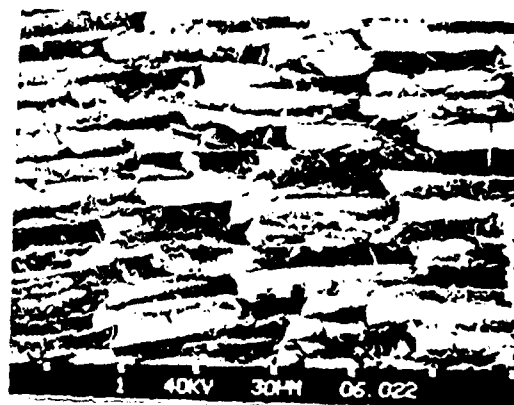
Fig. 3.21 Uncoated Glass-Epoxy (Rafael) after 200 g.
Sand impacted at 30° (30X and 1000X)
SEM Micrograph

A. General Appearance

B. Resin and Fibers Zones



A



B

Fig. 3.22 Uncoated Quartz-Polybutadiene after 200 g.
Sand impacted at 30° (500X and 500X)
SEM Micrograph

A. Resin Zone

B. Fibers Zone

3.3.2 Coatings.

Polyurethane coatings on E Glass epoxy and fluorocarbon coatings on quartz polyimide substrates were observed in the scanning electron microscope after being exposed to sand erosion conditions. The results are shown in Figure 3.23 to 3.29 and will be described herein for the various coatings.

-Polyurethane MIL-C-83286 on E Glass Epoxy

Typical general appearance of this coating's eroded surfaces is shown in Figure 3.23 and high magnification detailed eroded surface morphology is shown in Figure 3.24. Coatings surfaces exposed to normal impact angles at various constant amounts of sand particles are characterized by a cell type structure consisting of rounded cavities or craters up to 20-30 microns in size as can be seen in Figure 3.23B. The appearance of the surface did not change appreciably even with three times as much sand impacted.

The morphology of a coatings surface impacted with sand particles at 30° incident angle is shown in Figure 3.23C. The surface is characterized by elongated grooves and craters in the range of 30 μm indicative of local material removal.

A detailed picture of local erosion processes can be seen in Figure 3.24 for impact sand amounts of 200 gr, 600 gr at impact angles of 30° and 90°. Figure 3.24A shows that local material removal was associated with formation of cracks, crack propagation and intersection which resulted in removal of fragments of coatings materials in the range up to 10 microns. Moreover, these local erosion processes at normal

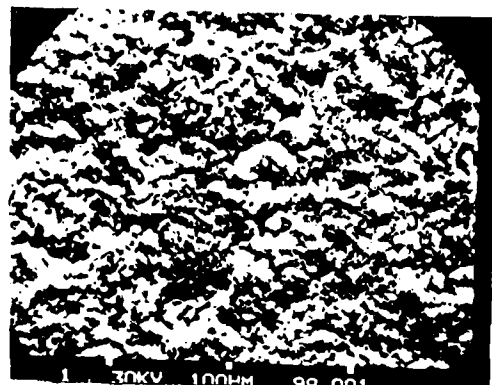
angles and material removal were associated with embedment of sand particles and fragments as can be seen in Figure 3.24C. Again note that the erosion after 600 gr sand impacted is only slightly larger craters compared to 200 gr eroded surfaces.

A crater formed by sand impacted at 30° angle on coating surface is shown in Figure 3.24B. The damage consists of several elongated craters around 30 microns in size. Also a fragment of a sand particle was found in the middle of the eroded area (Figure 3.24B).

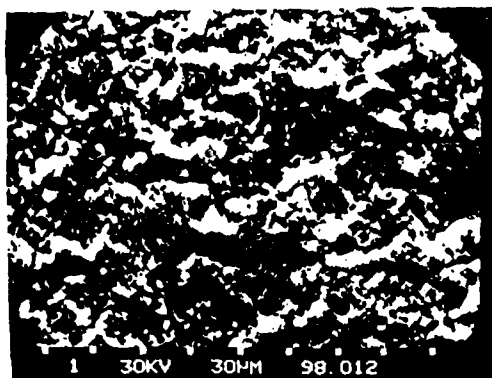
-Polyurethane MIL-C-83231 on Glass Epoxy

The general morphology and structure of eroded coatings surface as observed in scanning electron microscopy is shown in Figure 3.25. A typical unexposed coating surface is shown in Figure 3.25A. Exposure of coatings surface to erosion at low impact angles of 15° and 30° resulted in local material removal processes characterized by elongated craters up to 50 microns in length as can be seen in Figures 3.25B and 3.25C, respectively. Coatings surface impacted by sand particles at 90° was hardly damaged as shown in Figure 3.25D. Furthermore, even high magnification of the eroded coating surface at 90° did not reveal substantial damage in terms of material removal (See Figure 3.26B).

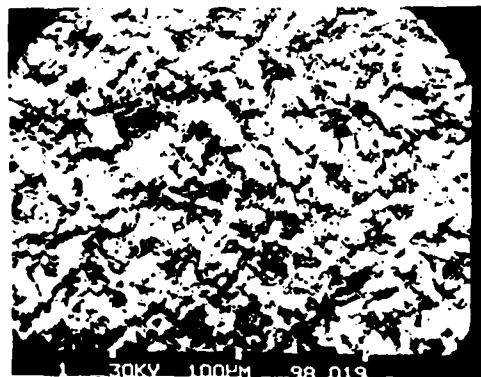
However, high magnification of the eroded area at 30° showed local material removal processes associated with cracks and fragments of material in the range of three microns and above. Figure 3.27 shows coatings surface morphology after being exposed to 600 gr sand particles at normal incidence angle. Under these conditions, no appreciable material removal processes were observed. Coatings surfaces were found



A

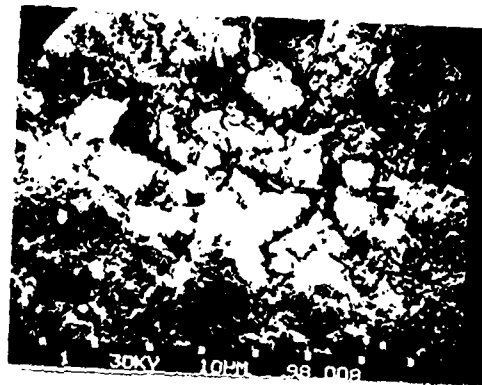


B

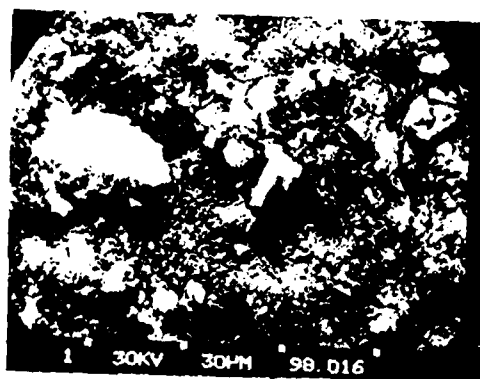


C

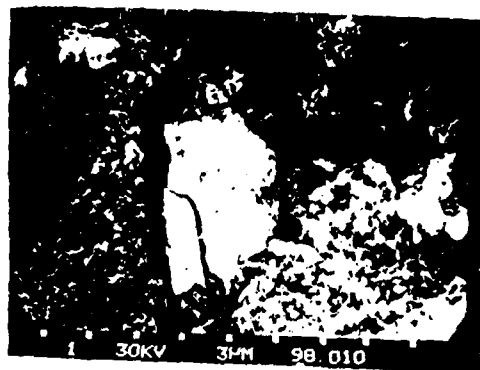
Fig. 3.23 MIL-C-83286 Polyurethane Coating on E Glass Epoxy Substrate after Sand Impact. A. 200 gr. 90°, B. 600 gr. 90°, and C. 200g. at 30°. 300x, 300x, and 250x SEM Micrograph



A

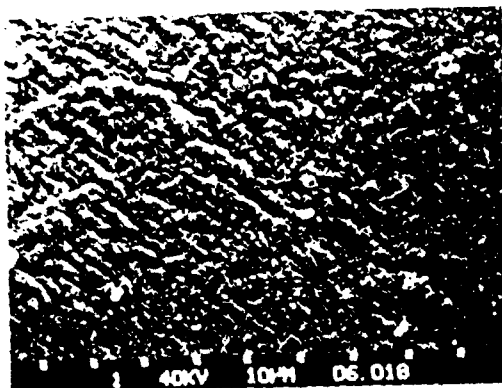


B

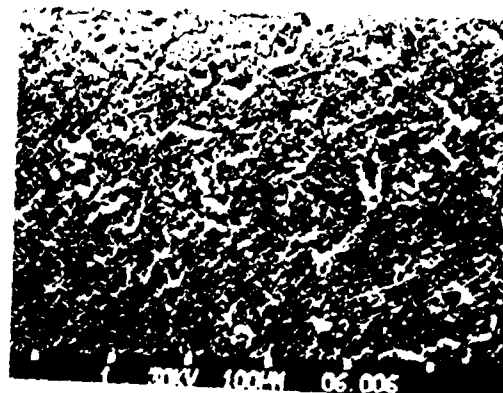


C

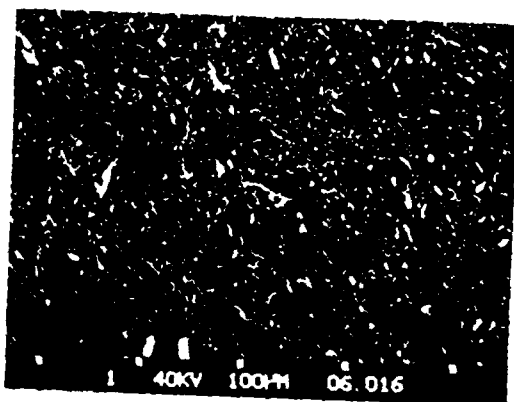
Fig. 3.24 MIL-C-83286 Polyurethane Coating on E Glass Epoxy Substrate after Sand Impact. A) 200g at 90°, B) 200g. at 30°, C) 600 g. at 90° (1000X, 600X, and 3000X)
SEM Micrograph



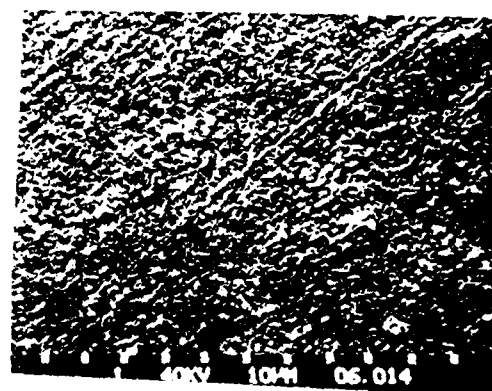
A



B

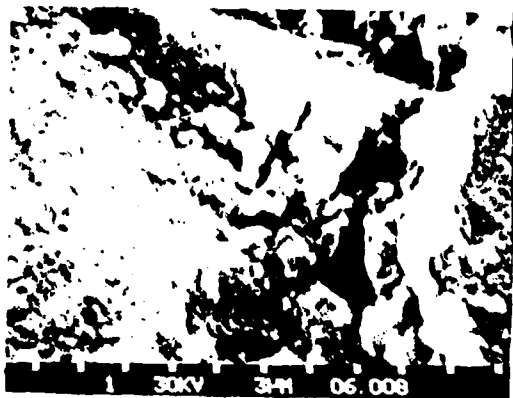


C

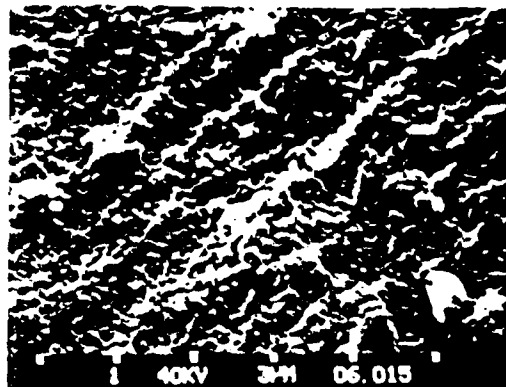


D

Fig. 3.25 MIL-C-83231 Polyurethane Coating on E Glass Epoxy
Substrate after Sand Impact A) Before erosion;
B) 200g. at 15° , C) 200g. at 30° , and D) 200g.
at 90° .
(1000X, 150X, 200X, 1000X)
SEM Micrograph



A



B

Fig. 3.26 MIL-C-83231 Polyurethane Coating on E Glass Epoxy
Substrate after Sand Impact: A) 200 g. at 15°
B) 200 g. at 90°
(3000X and 5000X)
SEM Micrograph

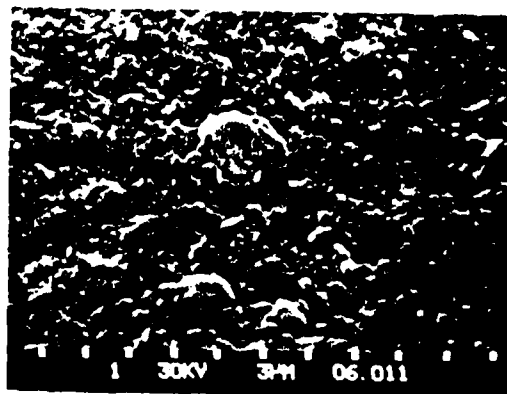
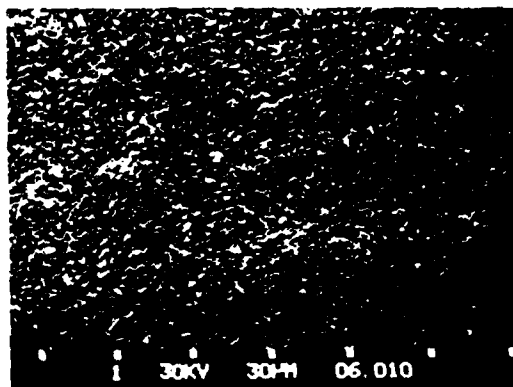


Fig. 3.27 MIL-C-83231 Polyurethane Coating on E Glass Epoxy
after 600 g. Sand Impacted at 90° (500 and 3000X)
SEM Micrograph

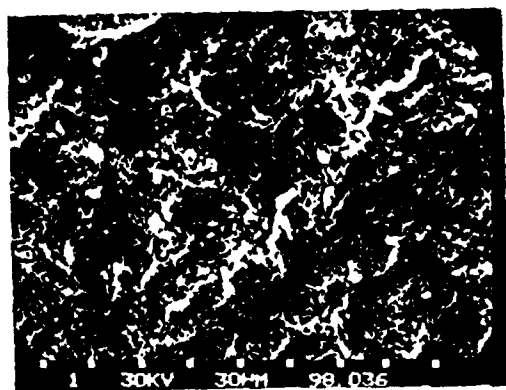
to be relatively smooth even in the micron scale as can be seen in Figure 3.27B.

-Fluorocarbon AF-C-VBW-15-15 Coatings on Quartz Polyimide Substrate

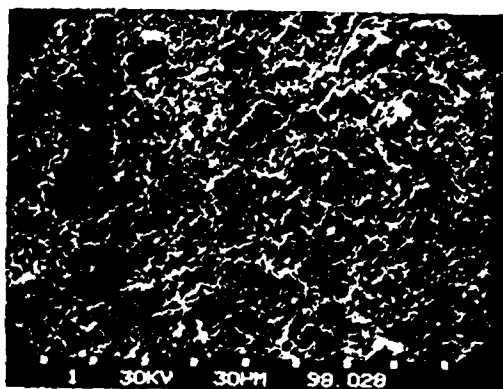
The morphology and structure of coatings surface after being exposed to 200 gr sand particles at 30° and 90° impact angles are shown in Figure 3.28. The general appearance of eroded surface at impact angles of 30° and 90° is shown in Figure 3.28A and Figure 3.28B, respectively. Both surfaces contained cracks and microcracks intersecting each other to form somewhat rounded and square type "grains" in the size range of up to 50 microns at 30° (Figure 3.28A) and 30 microns at 90° (Figure 3.28B).

High magnification observations of eroded surfaces showed how these cracks and microcracks propagated, intersecting each other and resulting in local removal of fragments of material from the coatings surface. These fragments could be as small as 1 micron (Figure 3.28D for impact angle of 90°) and as big as 10 or 30 microns (Figure 3.28C for impact angle of 30°).

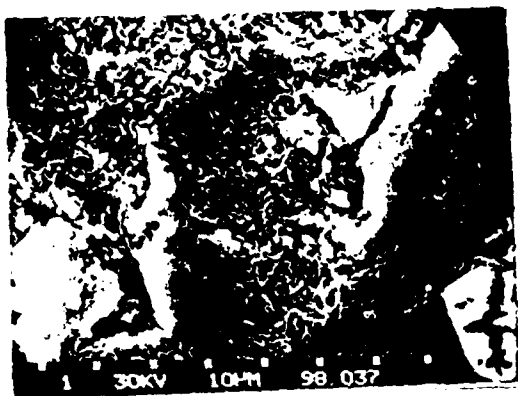
Impacting 600 gr sand particles at impact angle of 90° on surface coatings resulted in basically the same morphology and structure (Figure 3.29) as was observed when 200 gr impacted the surface (Figure 3.28B). At 600 gr few more craters and cavities in the range up to 30 microns in length were found (Figure 3.29D) as well as embedded fragments of sand particles in the range of 10-15 microns (Figure 3.29B).



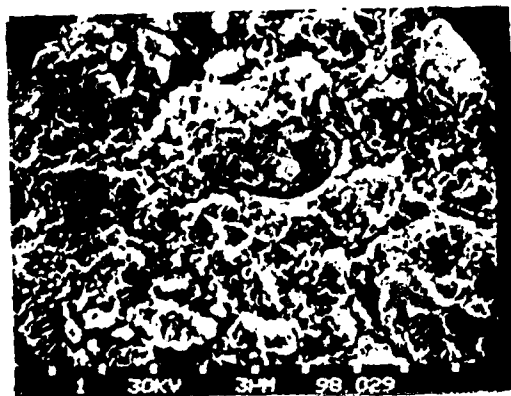
A



B

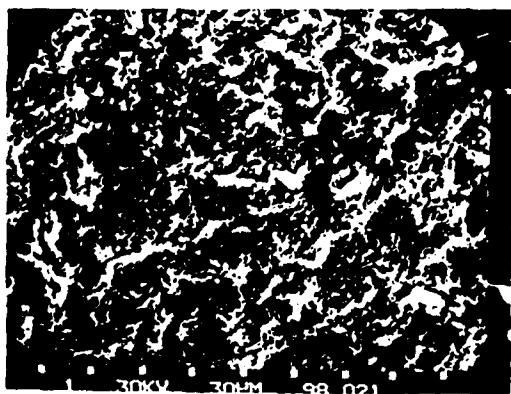


C

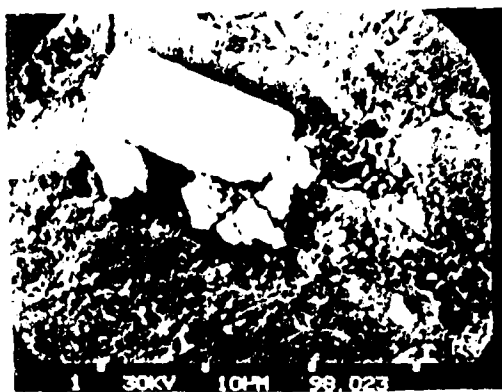


D

Fig. 3.28 AF-C-VBW-15-15 Fluorocarbon Coating on Quartz Polyimide Substrate after Sand Impact: A) 200g at 30°, B) 200g at 90°, C) 200g at 30°, D) 200g at 90° (300X, 300X, 1000X, and 3000X) SEM Micrograph



A



B

Fig 3.29: AF-C-VBW-15-15 Fluorocarbon Coating on
Quartz Polyimide Substrate after 600g
Sand Impacted at 90° (300X and 2000X)
SEM Micrograph

- A. General Appearance
- B. Embedded Sand Fragment in the Eroded Zone

4.0 Discussion

4.1 Composite Materials

The behavior of the composite materials was characterized by target weight change, surface roughness and surface structure and morphology.

4.1.1 Effect of Angle and Sand Weight Impacted

In previous investigations⁵ ductile materials showed maximum erosion or weight loss after being exposed to impact of solid particles at low incident angles in the range of $10-30^{\circ}$, while increasing the impact angles resulted in decrease of the erosion to a minimum value at normal angle.

On the other hand, so-called brittle materials showed minimum erosion at low incident impact angles. Erosion or target weight loss increased with increasing impact angle reaching a maximum value at normal angle.

The composite materials investigated (namely, Quartz polyimide, Glass Epoxy (RAFAEL) and Quartz polybutadiene) showed maximum erosion or weight loss at impact angles of 75° to 90° with 200 to 600 gr sand weight impacted (Figure 3.1, 3.3, 3.4). Minimum weight loss in these materials was found at the lowest impact angle of 30° . The data of target weight loss vs impact angle suggest therefore that the composite materials investigated behave as brittle materials under the sand erosion condition used in this research work. This is in keeping with their properties as thermosetting resins and inorganic fibers.

However, it was found that E Glass Epoxy material (supplied by AFWAL/MLBE) did not behave as so-called brittle material, but rather

as semi-ductile. In other words, maximum weight loss was obtained at impact angles around 45° for amounts of 200 gr, 400 gr, and 600 gr sand particles (Figure 3.2). Moreover, the weight losses of the E Glass Epoxy observed under these erosion conditions were lower by about one order of magnitude compared to values obtained in the other composite materials tested. This difference is likely due to the presence of higher percentage of glass fibers, better adhesion between the fibers and the resin as well as less porosity in the resin matrix.

The behavior of the composite materials tested; Quartz polyimide, Glass Epoxy and Quartz polybutadiene; under erosion conditions consisting of impacting various amounts of sand particles at constant angles was found to be the same. This behavior was characterized by progressive increase in target weight loss with increasing amounts of sand impacted. This was found⁵ also for glass and carbon reinforced nylon.

The rate of target weight loss versus amount of sand impacted was found to be fairly constant in the range of 0.4 to 0.6 mg/g at all impact angles. However, the average value of target weight loss versus amount of sand weight impacted was found to be around 0.1 mg/g for the E Glass Epoxy material supplied by AFWAL/MLBE. This low value is probably an indication that the weight loss in this material was basically due to removal of epoxy resin rather than to substantial removal of broken glass fibers (See Figure 3.19B).

Furthermore, if this composite material contains high percentage of fibers well adhered to the resin matrix and the main material removal is from the resin, then one would expect to find an overall

semi-ductile type behavior of the E Glass Epoxy target material (Figure 3.2) as was observed.

4.1.2 Surface Morphology

From observations of eroded surfaces in the scanning electron microscope, it appears that composite materials like Quartz-polyimide, Glass-Epoxy and Quartz-polybutadiene exhibit several stages of erosion and material removal processes. These stages can be characterized as follows:

- a) Local removal of resin material from the impacted surface resulted in exposing the fibers themselves to the erosive sand environment (Figure 3.19 for example).
- b) Solid sand particles impacting on the fibers causing their breakage through formation of cracks perpendicular to their length (Figure 3.22 for example).

These cracks across the fiber are caused by bending due to impact on the unsupported fibers since the matrix resin surrounding and supporting them has been removed. This has been observed previously^{12,13} in other types of composite materials under liquid impact.

- c) Further continuation of impact of the sand abrasive particles resulted in damaging the interface between the fibers and the resin matrix. This was characterized by the separation and detachment of broken fibers from the resin matrix (Figure 3.20 for example).

The morphology of eroded surfaces observed through the SEM suggest that the overall erosion damage of composite materials consist of matrix

material removal in the resin area (Figure 3.22), breakage and removal of broken fibers as well as removal of material from the fiber-resin interface zones (Figure 3.21). Differences in the erosion behavior of various types of composite material should be originated from the amount, type and properties of the fibers on one hand and from the type and properties of the resin material and its adhesion to the fibers on the other hand.

4.2 Coatings.

The sand erosion behavior of polyurethane and fluorocarbon coatings on composite material substrates was investigated by exposing coatings targets to varying amounts of flowing sand particles reaching the surface at various impact angles. The eroded coatings were then characterized by their weight change after erosion, their surface roughness (development), and their surface morphology as observed in the scanning electron microscope.

4.2.1 Effects of Angle and Sand Weight Impacted.

From studies of the impact angle, dependence of erosion on coating target weight loss, it appears that coatings such as polyurethane MIC-C-83286 on glass epoxy were affected substantially by the impact angle. This coating exhibits ductile behavior because maximum erosion occurs at low incident angle of 30° whereas minimum erosion occurs at normal angle. Furthermore, the weight loss of this polyurethane coating increased with increasing sand weight impacted in such a manner that for low incident angle of 30° the average rate of target weight

loss versus amount weight impacted was maximum and thereafter decreased with increasing impact angle reaching a minimum rate at 90° (Figure 3.11).

Elastomeric coatings materials like polyurethane MIL-C-83231 and fluorocarbon AF-C-VBW-15-15 were also affected by impact angle. For low incident angles of 15° and 30° , target weight loss was maximum but it was reduced to a minimum (near zero) at 30° - 45° . At higher impact angles from 45° to 90° , only weight gain was observed and this was independent of impact angle in the case of the polyurethane material (Figure 3.9 and 3.10). This weight suggests the embedment of sand particle fragments at the target eroded surface. Furthermore, the effect of amount of sand impacted on target weight loss showed that at impact angles in the range 45° to 90° , the target material gained weight rather than lost, independent of amounts of sand weight impacted (Figure 3.12 and 3.13).

However, at low incident impact angles of 15° and 30° , target weight loss increased with increasing sand weight impacted. The rate of target weight loss versus amount of sand impacted was rather small for the MIL-C-83231 polyurethane and AF-C-VBW-15-15 Fluorocarbon compared to the MIL-C-83286 Polyurethane (Figure 3.11).

In view of the polyurethane and fluorocarbon coatings' erosion resistance, these have been used as protective surface coatings on composite materials like E Glass-Epoxy and Quartz polyimide.

A comparison of uncoated E Glass-Epoxy and MIL-C-83286 and MIL-C-83231 Polyurethane coated E Glass-Epoxy and of uncoated Quartz-polyimide and AF-C-VBW-15-15 Fluorocarbon-coated Quartz-polyimide is shown in Figure 4.1 as a function of sand impacted at 30° angle. Note that the

- ◇ QUARTZ POLYIMIDE
- ▽ E GLASS EPOXY SUBSTRATE (AFWAL/MLBE)
- △ MIL-C-83286 POLYURETHANE COATING
- MIL-C-83231 POLYURETHANE COATING
- AF-C-VBW-15-15 FLUOROCARBON COATING

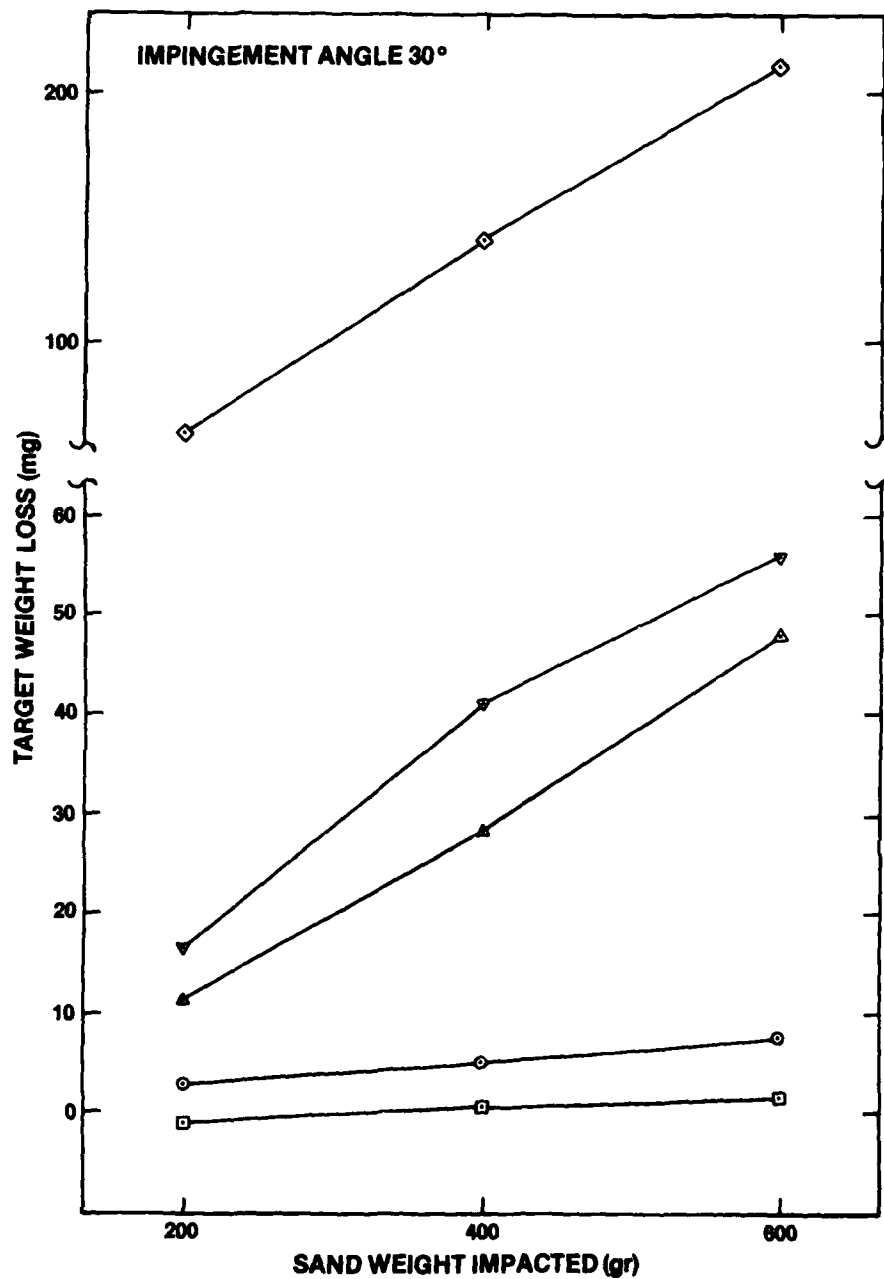


Fig. 4.1 Target Weight Change as Function of Sand Weight Impacted at constant impact angle of 30°.

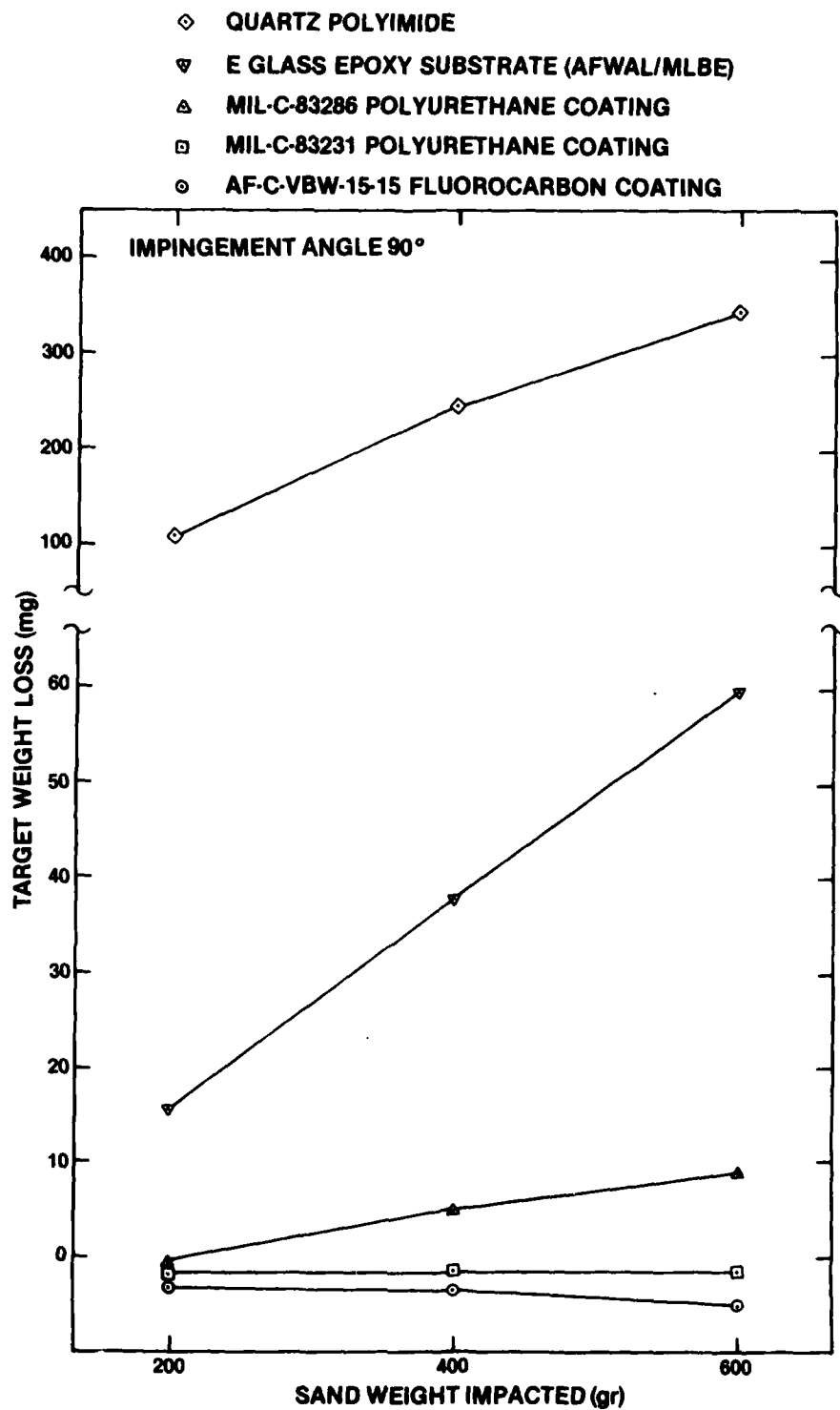


Fig. 4.2 Target Weight Change as Function of Sand Weight Impacted at constant normal impact angle.

Quartz-polyimide erosion is an order of magnitude greater than the E-Glass Epoxy and that the fluorocarbon erodes slightly more than the polyurethane. Figure 4.2 makes the same comparisons at a 90° angle with similar relative performance for the materials. In every case, the ability of these elastomeric coatings to protect the composite substrates is demonstrated. The erosion mass loss of the uncoated composites and the MIL-C-83286 Polyurethane increase similarly while the erosion of the elastomeric coatings is almost independent of sand weight impacted.

As long as the coatings remain intact, the protection at 90° is excellent; however, if failure occurs, then erosion of the composite will be extreme. By contrast, at the low angles the resistance of the coatings is reduced (See Figure 3.9 and 3.10) but the relative resistance of the composite is greater so that erosion would not be as catastrophic if coating failure occurred.

4.2.2 Surface Roughness (Effects)

Surface roughness studies of eroded coatings showed an inter-relationship among erosion rate, impact angles, and coatings surface morphology. Polyurethane and fluorocarbon coatings showed maximum weight loss at low impact angles of 15° to 30° (Figures 3.8, 3.9, 3.10). When maximum target weight loss was found, a maximum surface roughness was measured; i.e., maximum surface roughness was measured of coatings exposed to low impact angles at various constant amounts of sand impacted (Figures 3.14, 3.15, 3.16). Furthermore, the higher the value of weight loss, the higher was the surface roughness.

The correlation between amount of coating target weight loss and eroded surface roughness can be explained by the microscopic observations of eroded zones. The mode of coatings erosion consisted of local material removal as well as detachment of coatings pieces from the substrate especially at low impact angles. This resulted in very rough surfaces (Figures 3.25, 3.26).

When erosion rate was found to be negligible at impact angles of 45° to 90° (Figures 3.9, 3.10) the surface roughness was also found to be of minimum value (Figures 3.15, 3.16). These low values of erosion rate together with minimum values of surface roughness are in accordance with the coatings surface morphology. At these conditions no removal of coatings pieces occurred resulted in relative uniform smooth coating surfaces (Figures 3.26B, 3.27, 3.28B).

4.2.3 Surface Morphology

Microscopic observations of eroded coatings surfaces highlight important information about the mode of erosion processes taking place upon solid particle impingement. Solid particle erosion processes of polyurethane and fluorocarbon coatings consisted of local material removal processes in the size of up to 10 microns (Figure 3.24). Further examinations of coatings eroded surface indicated that upon solid particle impingements, local microcracks were formed, propagated and intersected each other causing the formation of local coating fragments both at low and high impact angles (Figure 3.24, 3.26A, 3.28).

The advanced stage of coating fragments removal from the eroded surface depended on the quality of the adhesion between the

coatings and the substrate. However, it was also dependent on the impact angle. At normal impact angle, the final removal rate was very low (Figures 3.28B, 3.28D, 3.24A) compared to high rate removal at low impact angles (Figures 3.24B, 3.25B, 3.26A). Also, it might be noted that at low impact angles, the removal of coatings material resulted in local elongated type craters or cavities at the eroded surface (Figure 3.25B).

In view of the results obtained by examination of eroded coatings surfaces, it can be deduced that the erosion processes consisted of several stages: a) formation of local microcracks in the coating, b) progression and intersection of microcracks resulting in formation of fragments of coatings, c) detachment of these fragments from the substrate, d) final removal of fragments from local eroded areas.

5. Conclusions

Composite material such as Quartz/polyimide, Quartz/polybutadiene and Glass/Epoxy as well as coatings such as polyurethane on Glass/Epoxy and fluorocarbon on Quartz/polyimide were exposed to sand erosion. The observations and the results obtained and described in this work led to the following major conclusions.

5.1 Composite Materials

A. Erosion or target weight loss increased with increasing impact angle reaching a maximum around 75° while the lowest erosion value was around 30° for various constant amounts of sand particles impacted.

B. At constant impact angle erosion rate or target weight loss increased progressively with increasing the amounts of sand weight impacted in the range of 200 gr to 600 gr.

C. The overall erosion processes taking place in these composite materials consisted of the following: (1) erosion or local material removal in the resin zones, (2) erosion in the fiber zones associated with breaking down the fibers into small fragments of 10 to 30 microns in length, (3) erosion of the interface zones between fibers and the adjacent resin matrix.

5.2 Coating Materials

A. In all coatings investigated, erosion rate (i.e., target weight loss) decreased with the increase of the impact angle. Maximum weight loss was found at 30° while minimum value of weight loss was found at

normal impact angle. However, in elastomeric MIL-C-83231 polyurethane and AF-C-VBW-15-15 fluorocarbon coatings, erosion rate was found to be independent of impact angle at the range of 45° to 90° .

B. A progressive increase in target coating weight loss with amount of sand impacted was found in MIL-C-83286 polyurethane coatings at constant impact angles.

C. In MIL-C-83231 polyurethane and AF-C-VBW-15-15 fluorocarbon coatings, erosion rate (i.e., target weight change) was found to be independent of weight of sand impacted at constant impact angles of 45° to 90° .

D. Eroded coatings surface roughness was found to follow target weight loss: The higher the weight loss, the higher the value of surface roughness observed.

E. Erosion processes in the coatings were associated with formation of microcracks, microcrack propagation and intersection resulting in fragments of coatings which were then locally removed from the surface.

REFERENCES

1. G. Hoff, G. Langbein, and H. Rieger, "Material Destruction Due to Liquid Impact," Erosion by Cavitation or Impingement, ASTM STP 408, American Society for Testing and Materials, 1967, pp. 42-69.
2. G. F. Schmitt, "The Erosion Behavior of Polymeric Coatings and Compositives at Subsonic Velocities," Proceedings of Third International Conference on Rain Erosion and Associated Phenomena, A. A. Fyall and R. B. King, Eds., Royal Aircraft Establishment, Farnborough, England, 1970, pp. 107-128.
3. A. A. Fyall, "Rain Erosion--A Special Radome Problem," Radome Engineering Handbook--Design and Principles, J. D. Walton, Ed., Chapter 8, Marcel Dekker, Inc., New York, 1970, pp. 461-562.
4. G. F. Schmitt, "Advanced Rain Erosion Resistant Coating Materials," Science of Advanced Materials and Process Engineering Series, Vol. 18, Society for Advancement of Materials and Process Engineering, 1973, pp. 57-75.
5. G. P. Tilly, "Erosion Caused by Airborne Particles," Wear, Vol. 14, No. 1, 1969, pp. 63-79.
6. G. P. Tilly, "Sand Erosion of Metals and Plastics: A Brief Review," Wear, Vol. 14, No. 4, 1969, pp. 241-248.
7. G. P. Tilly and W. Sage, "The Interaction of Particle and Material Behavior in Erosion Processes," Wear, Vol. 16, No. 6, 1970, pp. 447-466.
8. Neilson, J. H. and Gilchrist, A., Wear, Vol. 11, 1968, pp. 123-143.
9. Ruff, A. W. and Ives, L. K., Wear, Vol. 35, 1975, pp. 195-199.

10. Goodwin, J. E., Sage, W. and Tilly, G. P., Proceedings, The Institute of Mechanical Engineers, Vol. 184, Part 1, No. 15, 1959-1970, pp. 279-292.
11. Broadston, J. A. in Tool Engineers Handbook, 2nd ed., McGraw-Hill, New York, 1959, Section 89, pp. 1-5.
12. G. F. Schmitt, Jr., "Materials Parameters that Govern the Erosion Behavior of Polymeric Composites in Subsonic Rain Environments," Composite Materials: Testing and Design (Third Conference), ASTM Stp 546, American Society for Testing and Materials, 1974, pp. 303-323.
13. E. Van Rensen, "The Behavior of Fiber Materials Under Erosion and Cavitation Stresses," Proc. 4th International Conference on Rain Erosion and Associated Phenomena, A. A. Fyall and R. G. King, Eds., Royal Aircraft Establishment Farnborough, England, 1974, pp. 485-512.

APPENDIX A

EROSION DATA OF COMPOSITE MATERIALS

TABLE A.1
WEIGHT LOSS DATA FOR QUARTZ POLYIMIDE COMPOSITE

Amount of Sand Impacted (gr)	Impingement Angle (degrees)	Target Weight Loss (mg)	Average Weight Loss (mg)	Average * Erosion $\epsilon \cdot 10^6$
200	30	64.4 62.4	63.4	317.0
	45	75.5	95.5	477.5
	60	100.3 75.9	98.7	490.5
	75	111.4	111.4	557.0
	90	109.6 104.8	107.2	536.0
400	30	147.6 132.4	140.0	350.0
	45	206.0	206.0	515.0
	60	212.2 223.1	217.6	544.0
	75	246.5	246.5	616.2
	90	235.2 214.5	225.1	562.7
600	30	213.0 206.3	207.6	349.3
	45	284.7	284.7	474.5
	60	333.6 343.5	338.5	564.2
	75	346.3	346.3	577.2
	90	343.5 321.0	332.2	553.7

*Amount of material removed/amount of sand impacted.

TABLE A.2
WEIGHT LOSS DATA FOR AFWAL/MLBE E-GLASS EPOXY

Amount of Sand Impacted (gr)	Impingement Angle (degrees)	Target Weight Loss (mg)	Average Weight Loss (mg)	Average * Erosion $\epsilon \cdot 10^6$
200	30	15.0 18.0	16.5	82.5
	45	18.1	18.1	90.5
	60	16.8 20.5	18.6	93.0
	75	16.2	16.2	81.0
	90	14.8 15.7	15.2	76.0
400	30	40.9 42.1	41.5	103.7
	45	42.8	42.8	107.0
	60	40.2 43.8	42.0	105.0
	75	42.1	42.1	105.2
	90	34.2 41.3	37.7	94.2
600	30	60.8 52.3	56.5	94.2
	45	78.7	78.7	131.2
	60	73.1 66.7	69.9	116.5
	75	60.9	60.9	101.5
	90	59.4 59.7	59.5	99.2

*Amount of material removed/amount of sand impacted.

TABLE A.3
WEIGHT LOSS DATA FOR RAFAEL GLASS-EPOXY

Amount of Sand Impacted (gr)	Impingement Angle (degrees)	Target Weight Loss (mg)	Average* Erosion $\epsilon \cdot 10^6$
200	30	43.9	219.5
	45	59.5	297.5
	60	83.3	416.5
	75	80.0	400.0
	90	75.2	316.0
400	30	96.4	241.0
	45	147.1	367.7
	60	159.6	399.0
	75	169.3	423.2
	90	166.7	416.8
600	30	161.6	269.3
	45	175.5	292.5
	60	232.8	388.0
	75	202.0	336.6
	90	230.8	384.6

*Amount of material removed/amount of sand impacted.

TABLE A.4
WEIGHT LOSS DATA FOR QUARTZ-POLYBUTADIENE

Amount of Sand Impacted (gr)	Impingement Angle (degrees)	Target Weight Loss (mg)	Average Weight Loss (mg)	Average * Erosion $\epsilon \cdot 10^6$
200	30	70.9 84.2	77.5	387.5
	45	99.4	99.4	497.0
	60	121.2 135.9	128.5	642.5
	75	142.1	142.1	710.5
	90	156.7 146.2	151.4	757.0
400	30	169.0 140.8	154.9	387.2
	45	228.9	228.9	592.2
	60	257.0 281.0	264.0	672.5
	75	247.9	247.9	619.7
	90	247.8 267.3	257.5	643.8
600	30	228.9 197.7	213.3	355.5
	45	290.3	290.3	483.8
	60	352.2 383.4	367.8	613.0
	75	428.7	428.7	714.5
	90	359.1 339.0	349.0	581.6

*Amount of material removed/amount of sand impacted.

APPENDIX B

EROSION DATA OF COATINGS

TABLE B.1
WEIGHT LOSS DATA FOR MIL-C-83286 POLYURETHANE ON E GLASS EPOXY

Amount of Sand Impacted (gr)	Impingement Angle (degrees)	Target Weight Loss (mg)	Average Weight Loss (mg)	Average* Erosion $\epsilon \cdot 10^6$
200	30	10.9 12.0	11.4	57.0
	45	2.4	7.4	37.0
	60	1.8 3.2	2.5	12.5
	75	1.9	1.9	9.5
	90	-0.5 -0.4	-0.5	-2.5
400	30	26.9 29.9	28.4	71.0
	45	12.3	17.3	43.2
	60	10.6 9.0	9.8	24.5
	75	7.1	7.1	17.7
	90	5.0 4.7	4.8	12.0
600	30	48.2 48.4	48.3	80.5
	45	31.5	31.5	52.5
	60	18.8 21.2	20.0	33.3
	75	12.4	12.4	20.6
	90	9.4 8.6	9.0	75.0

*Amount of material removed/amount of sand impacted.

TABLE B.2
WEIGHT LOSS DATA FOR MIL-C-83231 POLYURETHANE ON E GLASS EPOXY

Amount of Sand Impacted (gr)	Impingement Angle (degrees)	Target Weight Loss (mg)	Average Weight Loss (mg)	Average * Erosion $\epsilon \cdot 10^6$
200	15	2.8	2.8	14.0
	30	-1.0 -0.8	-0.9	-4.5
	45	-1.2	-1.2	-6.0
	60	-1.1 -1.2	-1.2	-6.0
	75	-1.0	-1.0	-5.0
	90	-1.3 -1.2	-1.3	-6.5
400	15	6.5	6.5	16.2
	30	0.8 0.6	0.7	1.7
	45	-0.9	-0.9	-2.2
	60	-1.5 -0.8	-1.2	-3.0
	75	-1.8	-1.8	-4.5
	90	-1.3 -1.4	-1.4	-3.5
600	15	9.4	9.4	15.7
	30	2.0 1.2	1.6	2.7
	45	-0.6	-0.6	-1.0
	60	-1.5 -0.9	-1.2	-2.0
	75	-1.2	-1.2	-2.0
	90	-1.5 -1.5	-1.5	-2.5

*Amount of material removed/amount of sand impacted.

TABLE B.3
WEIGHT LOSS DATA FOR AF-C-VBW-15-15 FLUOROCARBON ON QUARTZ-POLYIMIDE

Amount of Sand Impacted (gr)	Impingement Angle (degrees)	Target Weight Loss (mg)	Average Weight Loss (mg)	Average * Erosion $\epsilon \cdot 10^6$
200	30	3.5 2.5	3.0	15.0
	45	-0.7	-0.7	-3.5
	60	-1.6 -1.4	-1.5	-7.5
	75	-2.0	-2.0	-10.0
	90	-2.8 -3.2	-3.0	-15.0
400	30	5.3 4.7	5.0	12.5
	45	0.0	0.0	0.0
	60	-1.4 -2.5	-2.0	-5.0
	75	-2.9	-2.9	-7.2
	90	-3.2 -3.3	-3.3	-8.2
600	30	6.7 8.8	7.8	13.0
	45	0.9	0.9	1.5
	60	-2.0 -2.2	-2.1	-3.5
	75	-2.8	-2.8	-4.6
	90	-5.6 -4.6	-5.1	-8.5

*Amount of material removed/amount of sand impacted.

APPENDIX C

SURFACE ROUGHNESS DATA OF COATINGS

TABLE C.1
SURFACE ROUGHNESS DATA FOR MIL-C-83286 POLYURETHANE/E GLASS EPOXY

Amount of Sand Impacted (gr)	Impingement Angle (degrees)	Roughness C.L.A. (microns)					Average
200	30	1.85	2.0	1.9	1.85	1.95	1.91 \pm 0.07
	45	2.25	2.1	2.0	2.1	2.2	2.13 \pm 0.10
	60	1.65	1.5	1.65	1.6	1.75	1.63 \pm 0.09
	75	1.3	1.25	1.35	1.25	1.1	1.25 \pm 0.09
	90	1.35	1.2	1.0	1.1	1.4	1.21 \pm 0.17
400	30	2.0	2.15	2.3	2.4	2.0	2.17 \pm 0.18
	45	2.0	1.85	2.7	2.1	1.85	1.90 \pm 0.15
	60	2.05	2.15	1.8	1.8	2.0	1.96 \pm 0.16
	75	1.55	1.65	1.4	1.35	1.5	1.49 \pm 0.12
	90	1.35	1.3	1.1	1.5	1.4	1.33 \pm 0.15
600	30	2.35	2.4	1.95	2.0	2.3	2.20 \pm 0.21
	45	2.35	2.1	2.4	2.3	2.5	2.33 \pm 0.15
	60	1.9	1.85	1.7	1.9	1.9	1.85 \pm 0.09
	75	1.45	1.75	1.65	1.6	1.6	1.61 \pm 0.11
	90	1.25	1.4	1.3	1.4	1.35	1.34 \pm 0.06
Before Erosion		0.08	0.14	0.23	0.11	0.17	0.15 \pm 0.06

TABLE C.2
SURFACE ROUGHNESS DATA FOR MIL-C-83231 POLYURETHANE/E-GLASS EPOXY

Amount of Sand Impacted (gr)	Impingement Angle (degrees)	Roughness (microns)					Average
		C.L.A.					
200	15	0.40	0.35	0.40	0.33	0.38	0.37+ 0.03
	30	0.28	0.28	0.27	0.24	0.28	0.27+ 0.02
	45	0.30	0.26	0.37	0.28	0.22	0.29+ 0.06
	60	0.22	0.21	0.28	0.23	0.22	0.23+ 0.03
	75	0.22	0.25	0.22	0.25	0.31	0.25+ 0.04
	90	0.30	0.28	0.29	0.22	0.30	0.28+ 0.03
400	15	0.60	0.66	0.62	0.70	0.76	0.67+ 0.05
	30	0.33	0.48	0.43	0.38	0.38	0.40+ 0.06
	45	0.32	0.34	0.27	0.28	0.32	0.31+ 0.03
	60	0.23	0.30	0.26	0.27	0.26	0.26+ 0.02
	75	0.26	0.20	0.20	0.32	0.28	0.25+ 0.05
	90	0.23	0.30	0.23	0.33	0.22	0.26+ 0.05
600	15	1.00	1.05	1.10	0.90	1.15	1.04+ 0.10
	30	0.55	0.47	0.45	0.55	0.50	0.50+ 0.05
	45	0.33	0.28	0.36	0.33	0.28	0.32+ 0.03
	60	0.26	0.30	0.21	0.21	0.24	0.24+ 0.04
	75	0.26	0.30	0.25	0.25	0.22	0.26+ 0.03
	90	0.25	0.35	0.37	0.30	0.32	0.32+ 0.05
Before Erosion		0.35	0.15	0.20	0.20	0.23	0.23+ 0.07

TABLE C.3
SURFACE ROUGHNESS DATA FOR AF-C-VBW-15-15 FLUOROCARBON/QUARTZ-POLYIMIDE

Amount of Sand Impacted (gr)	Impingement Angle (degrees)	Roughness					Average
		C.L.A.		(microns)			
200	30	1.05	1.2	1.1	1.0	1.15	1.0+ 0.08
	45	0.85	0.65	0.75	0.7	0.6	0.71+ 0.10
	60	0.6	0.85	0.65	0.75	0.5	0.67+ 0.13
	75	0.75	0.6	0.7	0.7	0.9	0.73+ 0.11
	90	0.75	0.6	0.85	0.55	0.8	0.11+ 0.13
400	30	1.25	1.5	1.65	1.5	1.35	0.45+ 0.15
	45	0.7	0.75	0.85	0.8	0.75	0.81+ 0.06
	60	0.6	0.75	0.6	0.75	0.65	0.67+ 0.08
	75	0.75	0.75	0.6	1.0	0.7	0.76+ 0.15
	90	0.95	0.8	0.85	1.1	0.75	0.74+ -.14
600	30	1.75	1.75	1.45	1.6	1.6	1.63+ 0.13
	45	1.0	0.7	0.65	0.7	0.85	0.78+ 0.14
	60	1.0	0.7	0.7	0.75	0.85	0.80+ 0.13
	75	0.9	0.8	0.6	0.65	0.6	0.71+ 0.13
	90	0.85	0.9	0.75	0.95	0.9	0.87+ 0.08
Before Erosion		0.35	0.40	0.55	0.44	0.35	0.42+ 0.08